Summer 8-31-2004

Characterization of mechanical behavior of electrospun non-woven mats

Ajitha Patlolla
New Jersey Institute of Technology

ABSTRACT

CHARACTERIZATION OF MECHANICAL BEHAVIOR OF ELECTROSPUN NONWOVEN MATS

by

Ajitha Patlolla

Electrospinning is a simple and efficient method for the production of nanometer to micrometer fibers. While the process of electrospinning has been known for over half a century, current understanding of the process and those parameters that affect the properties of the fibers is very limited. Not much work has been done in the field electrospinning process to study the mechanical properties of nonwoven mats produced and to study parameters affecting their properties.

In the first part of this thesis electrospun nonwoven mats made of poly(lactides) solutions were characterized based on their mechanical behavior in biorelevant conditions. In the second part of this thesis the effect of aging of solution on the mechanical behavior of electrospun nonwoven mats was investigated using poly(ϵ-caprolactone) as the solute.

The yield strain of the mat has increased in biorelevent conditions compared to ordinary conditions though no significant difference in yield strength was observed. The yield strength of the aged solution mat was less than that of fresh solution mat and also its mechanical behavior has changed completely.

CHARACTERIZATION OF MECHANICAL BEHAVIOR OF ELECTROSPUN NON-WOVEN MATS

by
Ajitha Patlolla

A Thesis
Submitted to the Faculty of
New Jersey Institute of Technology
in Partial Fulfillment of the Requirements for the Degree of
Master of Science in Biomedical Engineering
Department of Biomedical Engineering

August 2004

APPROVAL PAGE

CHARACTERIZATION OF MECHANICAL BEHAVIOR OF ELECTROSPUN NONWOVEN MATS

Ajitha Patlolla

Dr. Michael Jaffe, Thesis Advisor — Date
Research Professor, Biomedical Engineering Department, NJIT

Dr. Treena Arinzeh, Committee Member — Date
Assistant Professor, Biomedical Engineering Department, NJIT

Dr. George Collins, Committee Member — Date
Visiting Scientist, NJIT

BIOGRAPHICAL SKETCH

Author: Ajitha Patlolla

Degree: Masters of Science

Date: August 2004

Undergraduate and Graduate Education:

- Master of Science in Biomedical Engineering,
  New Jersey Institute of Technology, Newark, NJ 2004

- Bachelor of Science in Mechanical Engineering,
  Jawaharlal Nehru Technological University, Hyderabad, India, 1999

Major: Biomedical Engineering

This thesis is dedicated to my parents and husband

ACKNOWLEDGMENT

I would like to express my sincere gratitude to Dr. Michael Jaffe, for his faith, encouragement, guidance and financial support, throughout this research.

Special thanks to Dr. George Collins who has been guiding and helping me throughout my thesis.

I would like to thank Dr. Treena Arinzeh for her valuable suggestions and actively participating in my committee.

I also wish to thank Dr. Victor Tan, Head of Polymer Processing Institute who has helped me in thesis work; Joseph Pickton, lab manager for his assistance over the year; and Dr. Michael Dunn, research professor, UMDNJ for allowing me to use their equipment.

TABLE OF CONTENTS

TABLE OF CONTENTS
(Continued)

TABLE OF CONTENTS
(Continued)

Chapter **Page**

LIST OF TABLES

LIST OF FIGURES

LIST OF FIGURES
(Continued)

LIST OF FIGURES
(Continued)

Figure **Page**

CHAPTER 1

INTRODUCTION

A polymeric fiber is a polymer whose aspect ratio is greater than 100. The production of fibers from organic polymers involves forming the polymer into filaments and extending them uniaxially in order to orient molecules in the direction of the applied strain [1].

Human invention of the formation of polymeric fibers was achieved decades before the molecular structure of polymers was understood. It became evident in 1950s and 60s that the properties of polymers are strongly dependent on the physical organization of the macromolecules and on their chemical constitution. To form fibers from flexible-chain polymers, a randomly oriented melt or solution of the polymer must be converted into solid filaments having a high degree of preferred orientation along the fiber axis. The structural transformation achieved through various spinning and drawing methods, entails a number of complex molecular processes.

Fibers are the basic elements of nonwovens. Over the last 30 years the nonwovens industry fiber usage has grown by a factor of ten. Manufacturers of nonwovens can make use of any kind of fibers. Fiber requirements for nonwoven depends on the product being produced and the fabrication process being used, since each process leads to different range of fabrics properties, all available fibers cannot be used equally well in all nonwoven processes [2].

Conventional methods of polymer fiber production include melt spinning, solution spinning and gel state spinning. These methods rely on mechanical forces to produce fibers by extruding polymer melt or solution through a spinneret and subsequently drawing the resulting filaments as they solidify or coagulate. By using these methods, typical fiber diameters in the range of 5 to 500 microns can be produced. The consistently producible minimum fiber diameter is on the order of a micron [3].

Electrospinning is a unique method that produces polymer fibers with diameter in the range of nanometer to a few microns using electrically driven jet of polymer solution or melt [4, 5]. This technique has been developed since introduced by Formhals in 1934 [6]. It did not gain significant industrial importance in the past due to the low output of the process, inconsistent and low molecular orientation, poor mechanical properties and high diameter distribution of the electrospun fibers.

Development of electrospinning has been rapidly increasing in the past few years because it can prepare smaller than diameter of conventional fibers by 100 times. As compared to the conventionally used polymer fibers with micrometer scale, nanofibers have a high surface area-to-volume ratio. Hence, electrospun nanofibers have much potential in several bioengineering applications, such as tissue regeneration, biosensors, recognition and filtration of viruses and drug molecules [7, 8].

Mechanical properties of nonwoven mats used in clinical applications determine the responses of bodies to external mechanical influences for example the scaffold should

also have mechanically supportive properties for tissue regeneration while at the same time guiding cell differentiation and function. Mechanical properties of nonwoven fabrics depend on many parameters, including the properties of fibers and processing of nonwoven structure. Therefore it is important to review some of the elementary knowledge like fibers properties, web-processing technique etc. As size dimensions shrink the structure and architecture of these polymeric materials become crucial.

In this work, nanofibrous nonwoven mats were produced by electrospinning poly(lactides) and poly(ϵ-caprolactone) and their mechanical behaviors were characterized based on the parameters tested. The poly(lactides) chosen were poly(DL-lactide), poly(L-lactide), 85/15poly(DL-lactide-co-glycolide), and 50/50poly(DL-lactide-co-glycolide).

CHAPTER 2

BACKGROUND

A number of processing techniques such as drawing, template synthesis, phase separation, self-assembly, electrospinning, etc. have been used to prepare polymer nanofibers in recent years. According to Zheng-Ming Huang[9] the electrospinning process is the only method, which can be further developed for mass production of one-by-one continuous nanofibers from various polymers.

2.1 Electrospinning History

The electrostatic spray literature contains many helpful insights into the electrospinning process. Lord Raleigh [10] studied the instabilities that occur in electrically charged liquid droplets. He showed, over 100 years ago, that when the electrostatic force overcame the surface tension, a liquid jet was created. Zeleny [11] considered the role of surface instabilities in electrical discharges from drops. He published a series of papers around 1910 on discharges from charged drops falling in electric fields, and showed that, when the discharge began, the theoretical relations for the surface instability were satisfied. In 1952, Vonnegut and Neubaur [12] produced uniform streams of highly charged droplets with diameters of around 0.1mm, by applying potentials of 5 to 10 Kilovolts to liquids flowing from capillary tubes. Their experiment proved that monodisperse aerosols with a particle radius of a micron or less could be formed from pendent droplet at the end of the pipette. The diameter of the droplet was sensitive to the applied potential. Wachtel and coworkers [13] prepared emulsion particles using an

electrostatic method to make a monodisperse emulsion of oil in water. The diameters of the emulsion particles were from 0.5 to 1.6 microns. In 1960's Taylor [14] studied the disintegration of water droplets in an electric field. His theoretical papers demonstrated that a conical interface, with a semi-angle close to 49.3°, was the limiting stable shape.

Electrospinning of solutions of macromolecules can be traced back to 1934, when Formhals invented a process for making polymer fibers by using electrostatic force. Fibers were formed from a solution of cellulose acetate. The potential difference required depended on properties of the spinning solution such as molecular weight and viscosity. Formhals obtained a series of patents on his electrospinning inventions [15]

Gladding [16] and Simons [17] improved the electrospinning apparatus and produced more stable fibers. They used movable devices such as a continuous belt for collecting the fibers. Later, Bornat [18] patented another electrospinning apparatus that produced a removable sheath on a rotating mandrel. The basic principles were similar to previous patents. He determined that the tubular product obtained by electrospinning polyurethane materials in this way could be used for synthetic blood vessels and urinary ducts.

In 1971, electrospinning of acrylic fibers was described by Baumgarten [19]. Acrylic polymers were electrospun from dimethylformamide solution into fibers with diameters less than 1 micron. A stainless steel capillary tube was used to suspend the drop of polymer solution and the electrospun fibers were collected on a grounded metal screen.

Baumgarten observed relationships between fiber diameter, jet length, solution viscosity, feed rate of the solution and the composition of the surrounding gas.

In 1981, Manley and Larrondo [20] reported that continuous fibers of polyethylene and polypropylene could be electrospun from the melt, without mechanical forces. A drop of molten polymer was formed at the end of a capillary. A molten polymer jet was formed when high electric field was established at the surface of the polymer. The jet became thinner and then solidified into a continuous fiber. The molecules in the fiber were oriented by an amount similar to that found in conventional as-spun textile fibers before being drawn. The fiber diameter depended on the electric field, the operating temperature and the viscosity of the sample. X-ray diffraction and mechanical testing characterized the electrospun fibers. As either the applied electric field or the take-up velocity was increased, the diffraction rings became arcs, showing that the molecules were elongated along the fiber axis.

Reneker and coworkers [21] made further contributions to understanding the electrospinning process and characterizing the electrospun nanofibers in recent years. Doshi [22] made electrospun nanofibers, from water-soluble poly (ethylene oxide), with diameters of .05 to 5 microns. He described the electrospinning process, the processing conditions, fiber morphology and some possible uses of electrospun fibers. Srinivasan[23] electrospun a liquid crystal polyaramid, poly(p-phenylene terephthalamide), and an electrically conducting polymer, poly(aniline), each from solution in sulfuric acid. He observed electron diffraction patterns of polyaramid

nanofibers both as spun and after annealing at 400°C. Chun [24] used transmission electron microscopy, scanning electron microscopy and atomic force microscopy to characterize electrospun fibers of poly (ethylene terephthalate). Fang [25] electrospun DNA into nanofibers, some of which were beaded. Reneker and coworkers [26] also made carbon nanofibers, which had diameters from 50 to 500nm. The morphology ranged from highly oriented, crystalline nanofibers to very porous ones with high values of surface area per unit mass.

2.2 The Electrospinning Process

More than 50 patents for electrospinning polymer melts and solutions have been filed in the past 60 years [27]. However, there is no known commercial process for electrospinning. The manufacturing process of electrospinning was first reported by Formhals [15] in 1934. Since then, the process of electrospinning has caught the attention of many researchers and many reports, publications and patents in this field ascertain this. Gibson et al [16] describes electrospinning as a process in which high voltage is used to produce an interconnected membrane like web of small fibers. This method provides the capacity to lace together many types of polymers, fibers, and particles to produce ultra thin layers.

The electrospinning process is used to make fine fibers in the range of nano meters (which are also called nano fibers), by charging a polymer solution with several thousand volts. When sufficient voltage to overcome the surface tension is reached, fine jets of liquid are ejected towards a grounded object. The jet stretches and elongates as it travels

and is collected as an interconnected web like structure. Various publications indicate that the voltage required to produce fibers range from 5 kV to 30kV [28]. This range of voltage is good enough to overcome the surface tension of the polymeric solution and to produce very fine charged jets of liquid towards a grounded target. This charged jet before hitting the target undergoes splitting and drawing and forming fibers with different sizes and shapes before evaporating to form a web like structure.

The electrospinning system consists of two separate entities, a sprayer and a collecting device. The sprayer essentially consists of a glass or plastic syringe, which holds the polymer solution. One of the metal electrodes from the high voltage supply is applied to the solution, which serves as the positive terminal. A collector, which collects the fibers is given the other electrode, which serves as the negative terminal. In this process, polymer solution is charged to a very high electrical potential. Because of the electric field, charge is induced on the liquid surface. The presence of potential difference between the two electrodes causes a force opposite to the surface tension of the polymer solution. As the electric field increases, the hemispherical surface of the solution at the tip of the capillary tube (Figure 2.1[29]) extends to form a cone like structure, which is also known as the Taylor cone.

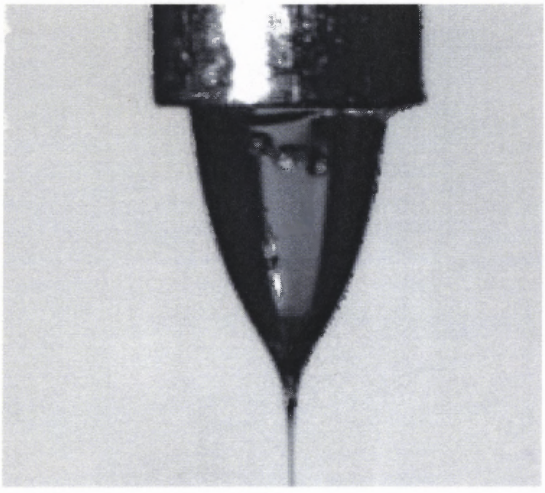

Figure 2.1 Taylor cone.

As the intensity of the electric field is further increased the field reaches a critical point value at which the repulsive electric force overcomes the surface tension force. At this point a charged jet of the solution is ejected from the tip of the Taylor cone. As the force acting on the polymer solution becomes greater than the surface tension, the charged droplet becomes unstable and this instability results in the formation of a charged jet. As this charged jet moves in the air, the solvent evaporate, leaving behind a charged polymer fiber, which lays itself randomly on a collecting plate. Fiber formation is due to the instability created by the repulsion between similar charges. Thus, continuous fibers are laid to form a web like structure.

So far in the open literature more than fifty different polymers have been successfully electrospun into ultra fine fibers. Many parameters can influence the transformation of polymer solutions into nanofibers through electrospinning. These parameters include (a) the solution properties such as viscosity, elasticity, conductivity, and surface tension,

(b)governing variables such as hydrostatic pressure in the capillary tube, electric potential at the capillary tip, and the gap (distance between the tip and the collecting screen), and (c) ambient parameters such as solution temperature, humidity, and air velocity in the electrospinning chamber [30].

Viscosity between 1–20 poises and surface tension between 35 and 55 dynes/cm are suitable for fiber formation. At viscosities above 20 poises, electrospinning was not possible because of the high cohesiveness of the solution. Droplets were formed when the viscosity was too low (<1 poise)[9].

Nanofibers obtained so far by this process are in the form of non-woven mats, which can be useful for relatively small number of applications such as filtration, tissue scaffolds, implant coating film, and wound dressing. However, from traditional fiber and textile industry, it is understood that only when continuous single nanofibers or uniaxial fiber bundles are obtained can their applications be expanded. This is a very tough target to be achieved for electrospun nanofibers, because the polymer jet trajectory is in a very complicated three-dimensional ''whipping'' way caused by bending instability rather than in a straight line. Efforts are being made in various research groups all over the world. Up to date, however, there is no continuous long nanofiber yarn obtained and the publications related to aligned nanofibers are very limited [9].

2.3 Common Biodegradable Polymers used in Electrospinning

Biodegradable polymers can be either natural or synthetic. In general, synthetic polymers offer greater advantages than natural materials because they can be tailored to give a wider range of properties and more predictable uniformity than can materials from natural sources. Synthetic polymers also represent a more reliable source of raw materials, one free from concerns of immunogenicity.

2.3.1 Poly(lactides)

Poly (Lactic acid) ---- **(- CO –CH(CH_3)-O-)$_n$**

Poly (glycolic acid) --- **(-CO-CH_2 –O-)$_n$**

Poly (lactic acid-co-glycolic acid) --- **(-CO-CH(CH3)-O-)$_x$- (-CO-CH2)$_y$-COOH**

Poly (glycolic) acid (PGA) and poly (lactic acid) (PLA) are aliphatic polyesters of poly(α-hydroxy acids). These polymers and their associated copolymers are perhaps the most common biodegradable synthetic polymers known and have been used in drug delivery, bone osteosynthesis and tissue engineering of skin [31].

PGA's relatively short chain length and polar properties give rise to its high crystallinity, melting point and low solubility in organic solvents [31]. PGA is also insoluble in the organic chloroform and dioxane solvents used in creating the scaffolds. This project is therefore unable to explore PGA polymer nonwoven webs.

As seen in the structures above, PLA has an extra chiral methyl group, making a D- or L-isomer possible. This extra methyl group also makes PLA more hydrophobic than PGA. PLA is hydrophobic and films of PLA take up only about 2% water [31]. Due to steric

hindrance of the methyl group, the ester bond of PLA is less likely to undergo hydrolysis, making the degradation time for PLA longer than its relative PGA and its copolymer PLGA. Other factors such as molecular weight, exposed surface area and crystallinity affect degradation rates as well [32]. P_LLA and $P_{DL}LA$ degrade by simple hydrolysis of the ester bond linkage to yield L-lactic acid or D-lactic acid, respectively.

Table 2.1 Common Properties of Poly(lactic acid)

	% crystallinity	Expected T_m (°C)	Expected T_g (°C)
P_LLA	37	185	57
$P_{DL}LA$	0	None	49

Because the L-lactic acid is a natural occurring stereoisomer of lactic acid, P_LLA is used more often than $P_{DL}LA$. However, crystallinity of the polymers also relates to their use. $P_{DL}LA$ is amorphous and therefore used in drug delivery applications that require uniform dispersion of species, while 37% crystalline PLA can often be found in orthopedic devices that require high mechanical strength and toughness [31].

Copolymers of GA and LA are known as PLGA have also been studied. PLGAs generally have lower T_m's and percent crystallnity than PGAs and increase rates of hydration and hydrolysis. Subsequently, they generally degrade more rapidly than PGA and PLA [32]. The hydrolysis reaction produces glycolic and lactic acids.

PGA and PLA copolymers all release acidic products upon hydrolytic degradation. In studies done on *in vivo* response of these polymers, about 8% of patients have shown late inflammatory reaction [32]. Acidic degradation products may contribute to the

inflammatory response and other polymers have been researched as a solution. One of these polymers is poly(ε-caprolactone), known as PCL [31].

2.3.2 Poly(ε -caprolactone)

Poly(ε-caprolactone) **(-CO-CH2- CH2- CH2- CH2- CH2-O-)n**

The degradation rate of PCL is much slower than PGA and has therefore been studied in controlled drug release systems and long-term implant devices. Its expected glass transition is around –66 °C and expected melting temperature is around 60°C.

PCL has some unusual properties, including a low T_g and T_m and a high thermal stability. These properties are related to PCL's chain of carbons, as longer chains give rise to lower T_m's and T_g's. PCL is also highly permeable, which results from its low T_g and subsequent rubbery state at room temperature [32].

PCL can degrade by several different mechanisms. As reported in Lanza et al., [32] PCL can undergo hydrolysis or enzymatic degradation. Currently, PCL can be found in a one-year implantable contraceptive device called Capronor and drug delivery devices. However research of potential use as an implant is ongoing.

2.4 Clinical Applications of Electrospun Mats

From a biological viewpoint, almost all of the human tissues and organs are deposited in nano fibrous forms or structures. Examples include: bone, dentin, collagen, cartilage, and skin. All of them are characterized by well-organized hierarchical fibrous structures

realigning in nanometer scale. According to the research conducted in the field of nanotechnology, compatibility has to do with the size of the fibers that make up the materials. As such, current research in electrospun polymer nanofibers has focused one of their major applications on bioengineering.

2.4.1 Medical Prostheses

Polymer nanofibers fabricated via electrospinning have been proposed for a number of soft tissue prostheses applications such as blood vessel, vascular, breast, etc. In addition, electrospun biocompatible polymer nanofibers can also be deposited as a thin porous film onto a hard tissue prosthetic device designed to be implanted into the human body. This coating film with gradient fibrous structure works as an interphase between the prosthetic device and the host tissues, and is expected to efficiently reduce the stiffness mismatch at the tissue/device interphase and hence prevent the device failure after the implantation[9].

2.4.2 Tissue Engineering

For the treatment of tissues or organs in malfunction in a human body, one of the challenges to the field of tissue engineering is the design of ideal scaffolds/synthetic matrices that can mimic the structure and biological functions of the natural extracellular matrix (ECM). Human cells can attach and organize well around fibers with diameters smaller than those of the cells. In this regard, nanoscale fibrous scaffolds can provide an optimal template for cells to seed, migrate, and grow. A successful regeneration of biological tissues and organs calls for the development of fibrous structures with fiber architectures beneficial for cell deposition and cell proliferation. Of particular interest in tissue engineering is the creation of reproducible and biocompatible three-dimensional

scaffolds for cell ingrowths resulting in bio-matrix composites for various tissue repair and replacement procedures. Recently, people have started to pay attention to making such scaffolds with synthetic biodegradable polymer nanofibers. It is believed that converting biopolymers into fibers and networks that mimic native structures will ultimately enhance the utility of these materials, as large diameter fibers do not mimic the morphological characteristics of the native fibrils [9].

2.4.3 Wound Dressing

Polymer nanofibers can also be used for the treatment of wounds or burns of a human skin, as well as designed for haemostatic devices with some unique characteristics. With the aid of electric field, fine fibers of biodegradable polymers can be directly sprayed/spun onto the injured location of skin to form a fibrous mat dressing which can let wounds heal by encouraging the formation of normal skin growth and eliminate the formation of scar tissue, which would occur in a traditional treatment. Non-woven nanofibrous membrane mats for wound dressing usually have pore sizes ranging from 500 nm to 1 mm, small enough to protect the wound from bacterial penetration via aerosol particle capturing mechanisms. High surface area of 5–100 m2/g is extremely efficient for fluid absorption and dermal delivery [9].

2.4.4 Drug Delivery and Pharmaceutical Composition

Delivery of drug/pharmaceuticals to patients in the most physiologically acceptable manner has always been an important concern in medicine. In general, the smaller the dimensions of the drug and the coating material required to encapsulate the drug, the

better the drug to be absorbed by human being. Drug delivery with polymer nanofibers is based on the principle that dissolution rate of a particulate drug increases with increasing surface area of both the drug and the corresponding carrier if needed. As the drug and carrier materials can be mixed together for electrospinning of nanofibers, the likely modes of the drug in the resulting nano structured products are: (1) drug as particles attached to the surface of the carrier which is in the form of nanofibers, (2) both drug and carrier are nanofiber-form, hence the end product will be the two kinds of nanofibers interlaced together, (3) the blend of drug and carrier materials integrated into one kind of fibers containing both components, and (4) the carrier material is electrospun into a tubular form in which the drug particles are encapsulated. The modes (3) and (4) are preferred. However, as the drug delivery in the form of nanofibers is still in the early stage exploration, a real delivery mode after production and efficiency have yet to be determined in the future [9].

2.5 Characterization of Nonwoven Mats

Although the concept the electrospinning dates back to many years from now, not much of characterization has been done in this field. The demand of these electrospun fibers in wide variety of applications has influenced to develop the characterization and testing techniques for the webs produced.

One of the foremost roles of the electrospinning process is to produce small diameter fibers. Almost everybody who has done electrospinning experiments has reported that the fibers spun through this process have fiber diameters in the range of a few 500

nanometers to a couple of microns. Fibers spun through different polymer solutions did not make much of a difference in the fiber diameter.

The measurement of fiber diameter in the electrospun webs that have been reported in the literature is based using various image analysis techniques. The instruments for measuring the fiber diameter and the analysis have been done using various instruments, mainly scanning electron microscope, transmission electron microscope and atomic force microscopes.

There is very little data available in the literature on the mechanical properties of electrospun nonwoven mats because not much work is done in this field [33]. It has been supposed that nanofibers can have better mechanical performance than microfibers [9]. Till now in the open literature no one has given information in detail regarding their mechanical properties and how the electrospinning process parameters affect their properties.

Many different methods can be used for testing non-woven mats but the only common test method, which can be used to determine fracture properties whether, the material is soft or hard, oriented or isotropic, brittle or highly extensible, is the simple tensile test. This suggests that the best basis for the classification of the short-term fracture behavior especially for fibers is the shape of stress strain curve.

In a tensile test, a sample of known dimensions (including thickness) is held between two clamps. As the sample is stretched, the force exerted by the instrument and the length (and sometimes cross-sectional area) of the sample is measured. This data can be used to construct a stress strain curve and to calculate several mechanical properties of the non-woven mat. The three important properties determined from the Stress Strain curve are Yield point, Tensile Strength and Modulus of Elasticity. Yielding is a phenomenon closely related to the onset of permanent deformation. This is due to molecular chains unfolding and becoming aligned in the direction of the applied load. Yield point in Stress-Strain curve is located as a point where the curve deviates from straight to curve. But for plastics yield point is defined at the point where the load begins to drop. The tensile strength is the stress needed to break the sample. The capacity of a material to resist elastic displacement under stress, which refers to the deformation behavior in the elastic region, is known as Modulus of elasticity or Young's modulus. It is the slope of a stress-strain curve. Stress-strain curves often are not straight-line plots, indicating that the modulus is changing with the amount of strain. In this case the initial slope usually is used as the modulus.

In biorelevant testing of polymer fibers the temperature of interest is limited to 37±3°C and it is the time effects in aqueous environment containing biological molecules that are critical [34].

CHAPTER 3

RESEARCH OBJECTIVE

This thesis was divided into two parts because while working on part I in the process of making nonwoven mats, it was observed that long standing solutions mats strength when pulled between the hands was different from that of newly prepared solution mats. This led to Part II of thesis for which a suitable experiment was designed.

The objective of first part of the thesis is to produce very fine fibers of poly(lactides) using electrospinning and to study their mechanical behavior in biorelevant conditions.

The objective of second part of the thesis is to investigate the effects of aging of solution on the mechanical behavior of nonwoven mats produced using electrospinning.

CHAPTER 4

EXPERIMENTAL DESIGN

This chapter explains the apparatus used for the electrospinning process, materials used, solution preparation, non-woven mat preparation and a complete picture of the characterization procedure.

4.1 Electrospinning Equipment Setup

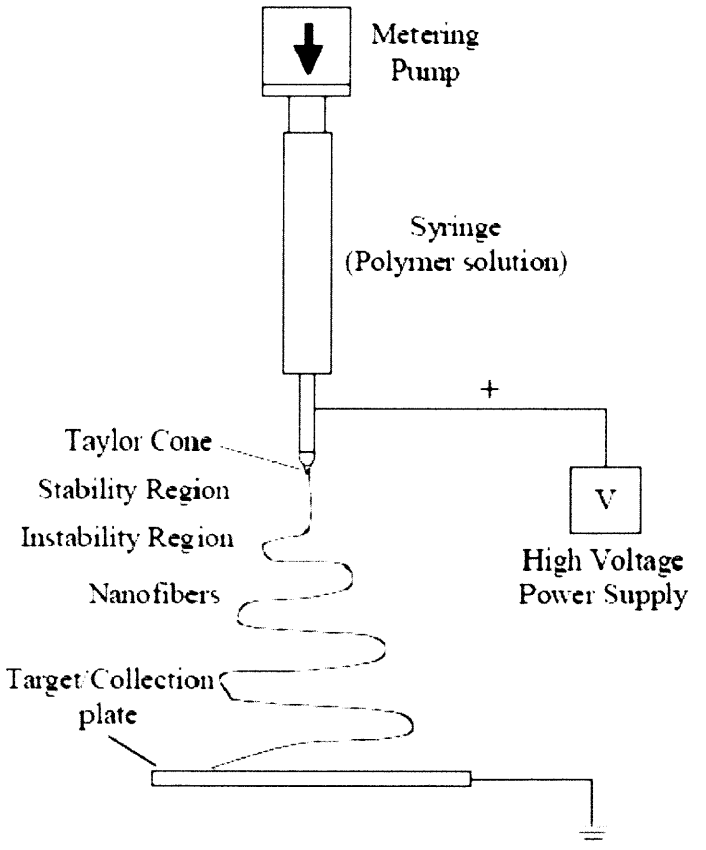

Figure 4.1 Schematic of electrospinning process showing the formation of nanofibers.

The basic elements of an electrospinning apparatus used are gamma high voltage (30KV) source (Ormond beach, FL), a collector (ground) electrode/mandrel (Steel alloy of 200mmL X 100mmW X 2mmH), a source electrode, and a polymer solution to be electrospun. The electrospinning source solution is prepared with the polymer of interest in an appropriate solvent at concentrations that support the formation of chain entanglements. The electrospinning solution can be delivered to the electric field in a syringe (plastic disposable 10ml syringe); various tip-bore configuration and diameters can be used with this approach. The positive output lead of a high-voltage supply is attached to the blunt needle (20 gauge) of the syringe reservoir. Charging the polymer solution to 15-30 KV draws, with the electric field as the driving force, the solvent containing the polymer. The solvent evaporates and the polymer fibrils form. The electrospinning setup is shown schematically in Figure 4.1 [35].

4.2 Materials

The materials used for electrospinning were biodegradable polyesters (PLA, PLGA and PCL) as solute and Methylene chloride as solvent. Samples were chosen such that they are around same molecular weight. They were received in the form of small 500gm sealed packets.

- All the poly (lactide-co-glycolide) polymers were purchased from Alkerms, Ohio.
  - $P_{DL}LA$ with inherent viscosity 0.55dL/g, Molecular weight 83kD, Polydispersity 1.7, glass transition 49.6 °C, Lot No: W2297-587 which was manufactured on 10/24/02.

- 85/15PLGA with inherent viscosity 0.63dL/g, Molecular weight 95kD, Polydispersity 1.6, glass transition 49.2 °C, Lot No: 9106-404 which was manufactured on April 1999.
- 50/50PLGA with inherent viscosity 0.76dL/g, Molecular weight 71kD, Polydispersity 1.69, glass transition 46.7 °C, Lot No: W3205-612 which was manufactured on 07-24-03

- PCL, Molecular weight 80,000 with glass transition –60°C from Aldrich Chemical Company Inc (Milwaukee, WI).
- PLLA was purchased from Boeringer.
- Methylene Chloride was purchased from Fisher Scientific

4.3 Solution Preparation

The solutions of PLA, PLGA and PCL were prepared in glassware using the following technique. Glassware was cleaned using an initial rinsing with tap water. The desired amount of polymer according to the concentration (weight/weight) required was weighed using Mettler AE100 closed balance. These polymer chips were poured into a glass bottle containing a Methylene chloride (dichloromethane), which is also being weighed using the balance. The glass bottle has to be closed by an airtight lid to maintain the concentration throughout. A homogeneous solution was achieved by heating and slow agitation using magnetic stirrer on heater and stirrer instrument (Fisher Scientific). All solutions were prepared at room temperature.

4.4 Viscosity of the Solution

Viscosity of the solution used for electrospinning was found using Rheometrics Rheometer and Brookfield Dial Viscometer (Stoughton, MA) RVTCP type (Figure 4.2).

Figure 4.2 Brookfield Viscometer.

The Brookfield Dial viscometer measures fluid viscosity at given shear rate. Viscosity is a measure of a fluid's resistance to flow. The dial viscometer rotates a sensing element in a fluid and measures the torque necessary to overcome the viscous resistance to the induced movement. This is accomplished by driving the immersed element, which is called spindle, through a beryllium copper string. The degree to which the spring is wound indicated by a red pointer, is proportional to the viscosity of the fluid. 1ml volume of the solution is used to find the viscosity based on the cone used.

4.5 Nonwoven Mats Preparation

Biodegradable polymers sample mats were prepared and were characterized. Constant processing conditions were maintained for all the samples made in order to compare their tensile properties. For all the samples the solvent used was methylene chloride. To determine the lower limit of polymer concentration, several runs were conducted. The

least possible concentration was used for all the polymers. The solution was loaded into a 10ml syringe plunger. A 20 gauge blunt needle of diameter .023"(.58mm) needle was then placed on the syringe to act as the electrospinning nozzle and charging point for the contained solution. The filled syringe was placed on a syringe set to dispense the solution at the rate of 0.5ml/min. The positive lead from the high-voltage supply was attached to the metallic part of the blunt needle. The syringe pump was turned on and the high-voltage supply was set at 30kV. The grounded target was a 303 stainless steel large mandrel (0.5cm H x 10 cm W x 20cm L) placed 20cm from the tip of the needle. The polymer solution was electrospun to form a large white mat on the grounded mandrel. The thickness of the mat produced can be increased or decreased by simply adjusting the amount of polymer electrospun by increasing the volume and electrospinning time. All the mats produced were almost of same of uniform thickness. Leave the mat on the mandrel for some time and then remove so that all the moisture dries. The mat was then processed for scanning electron microscopy (SEM) and Instron tensile testing.

4.6 Characterization of Nonwoven Mats

Nonwoven mats of biodegradable polymers were characterized based on morphology, tensile, and thermal properties. The morphology of the mats was studied using SEM, tensile properties using Instron and thermal properties using DSC and TGA.

The experimental design was divided into two parts based on the processing parameters and the polymers used. The influence of these parameters on the structural parameters and properties of the produced nanofiber web need to be revealed in order to produce

webs of predetermined properties for certain end use. The following sections describe the methods implemented to measure the morphology, mechanical and thermal properties of the nanofiber webs produced for this study.

4.6.1 Morphology

Understanding how the morphology is affected by solute used is essential to produce webs with desired properties. Images of nanofiber webs were captured by scanning electron microscopy (SEM) as a first step to determine fiber diameter and distribution.

The Scanning Electron Microscope is a microscope that uses electrons rather than light to form an image. There are many advantages to using the scanning electron microscopy over using the traditional light microscope. The scanning electron microscope has a large depth of field (enabling 3-dimensional observation), that allows several layers of the sample to be in focus at one time thus enable measurements of large number of fibers in an image. The SEM also produces images of high resolution, which means that closely spaced features can be examined at a high magnification. Preparation of the samples is relatively easy since most scanning electron microscopes only require the sample to be electrically conductive. The combination of higher magnification, larger depth of focus, greater resolution, and ease of sample observation makes the SEM the best choice for the study of electrospun fiber web structures. The operating principle of the scanning electron microscope can be illustrated as a finely focused electron probe made to scan the specimen surface. As a result of this, secondary electrons and backscattered electrons are emitted from the specimen surface, which are detected and fed to a synchronously

scanned cathode ray tube as an intensity-modulating signal. The signal thus received displays the specimen image on the cathode ray tube screen. Secondary electrons are low energy electrons emitted from the vicinity of the surface of specimen. Backscattered electrons are the electrons backscattered by specimen and having almost the same energy as that of incident electrons. These electrons contain two types of information: one on specimen composition and the other on specimen topography.

Figure 4.3 LEO 320 Scanning Electron Microscope.

The analyses of the electrospun webs were done with the help of LEO 1530 Field Emission SEM (Figure 4.3). The LEO 1530 is an ultra-high resolution field emission SEM utilizing the GEMINI field emission column. It is well suited to a wide range of applications due to its versatile specimen chamber and eucentric stage. Six free ports for

the attachment of optional detectors and accessories enable the instrument to be used as a complete analytical workstation.

The electrospun web samples used in this method were not coated. The SEM was interfaced with computer having LEO 320 software. Since the scanning electron microscope uses a high voltage for its operation and the electron beam is so sharp and intense that a small speck of dust in the system or in the sample may ruin the measurement of the whole sample. So proper care must be taken while preparing the sample and mounting the sample on the microscope. The samples for the scanning electron microscope can be prepared first of all by cleansing the sample holders (stubs). Cleaning the holders was done using a sonicator and acetone was used as the cleansing agent. It is then dried and a layer of sticky pad (double sticky tapes) is pasted to the stubs. Sample is cut into a shape of square of 4mmx4mm and stuck to the pad on the stub. The specimen fixed stubs was then mounted on the microscope chamber. To begin with the image capturing, proper spot size and accelerating voltage should be selected. Image was captured at a voltage of 3KV and a working distance of 6mm and at various magnifications. The images obtained could be stored with TIFF format in a zip disk.

In this experiment, range of the fiber diameter was determined by adjusting to the required magnification and identifying the small diameter nanofibers and large diameter nanofibers and then noting their values.

4.6.2 Tensile Properties

Nonwoven mats of 200mm X 100mm X .5mm of uniform thickness were prepared and cut into rectangular strips of 12mm width and 100mm height using JDC precision sample cutter (Thwing Albert Instrument Company, Philadelphia). From each mat 15 strips were formed and these were tested at room temperature.

Figure 4.4 Instron 5542 mechanical tensile tester.

Electrospun mats were subjected to stress-strain analysis using an Instron 5542 mechanical tensile tester (Figure 4.4). The Instron tensile tester measures basic mechanical properties of polymer samples. The instrument uses a load cell to stretch a sample at a set strain rate, while a load cell records the force as a function of strain. This

enables the following calculations: tensile strength, yield point, tensile modulus and other mechanical property data, tenacity of fibers, etc.

The software is Merlin. The maximum load cell was 100N. The initial gauge length was 50mm for lactides and 35mm for polycaprolactone, the width of the strip was 12mm and the thickness was .50mm for lactides and 0.2mm for polycaprolactone. The stress-strain analysis was conducted with the grips moving at a rate of 0.5 inch/min for lactides and 5 inch/min for PCL samples.

The procedure to be followed is:

- Measure the thickness of the specimen at several points along the length and note the least thickness of the sample.
- Based on the material the rate of grip separation was decided. For the material having percent elongation at break greater than 100% rate of grip separation was 5inch/min and for the material having percent elongation at break less than 20% grip separation was chosen to be 0.5 inch/min.
- Enter all the information in the computer before placing the sample in between the grips and then balance the load to 0.0 lbf.
- Place the strip in between the grips such that the load is nearly 0.0 lbf and start the machine, which then records the stress strain behavior of the sample.
- Five specimens were used for each set of polymer.

4.6.3 Biorelevant Testing of Tensile Properties

The samples were incubated in Phosphate Buffer Solution (PBS) with PH of 7.4 at a temperature of 37° C for 18 hours in a temperature control bath and then removed from the bath, and their tensile properties were tested similarly at room temperature using Instron.

4.6.4 Thermal Properties

Thermal analysis of the electrospun PCL web was carried out using TA Q100 Differential Scanning Calorimetry (DSC)(Figure 4.5), which is a heat flux type calorimetry and Thermogravimetric Analysis (TGA) TA Q50 (Figure 4.7).

Differential Scanning Calorimetry

Differential scanning calorimetry (DSC) measures the heat emission or absorption of the test material. In heat flux DSC, the sample and a reference substance are placed on a metal plate connected to a furnace acting as a heat sink, and the temperature difference between the test and reference substances is measured to calculate the heat flow. Since both samples are in a uniformly heated furnace, noises due to changes in temperature and convection are small, and the baseline is stable. Therefore, measurement sensitivity is high, which is typically up to 700°C, and down to -140°C with a liquid nitrogen cooling system.

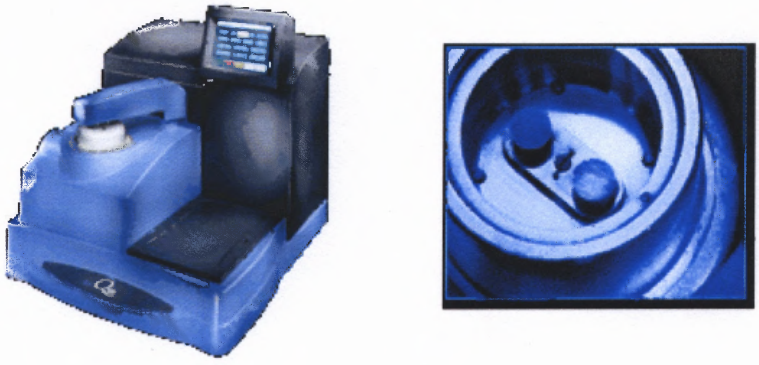

Figure 4.5 TA Q100 Differential Scanning Calorimetry.

DSC measures temperatures and heat flows associated with thermal transitions in a material. Common usage includes investigation, selection, comparison and end-use performance of materials in research, quality control and production applications. Properties measured include glass transitions, "cold" crystallization, phase changes, melting, crystallization, product stability, and oxidative stability.

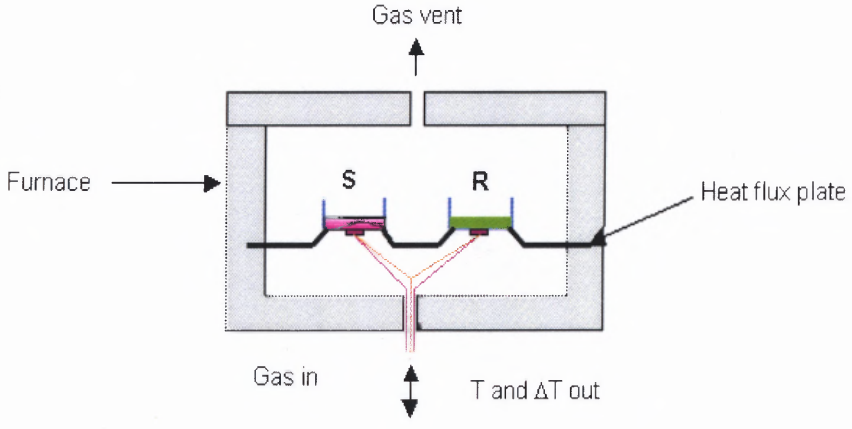

Figure 4.6 Schematic of DSC operation.

The system (Figure 4.6) uses aluminum pans for holding the sample/standard (S) and the reference (R). The equipment gives the output in terms of the thermogram curves and the following information can be obtained from these thermograms. It essentially provides the melting point, crystallization and glass transition temperature. The cooling options are ice water (0°C), intercooler (-60°C) or liquid nitrogen (-170°C).

The operation sequence of the equipment involves running the system base line to zero temperature, running the standard to calibrate temperature range and finally running the sample. In one of the pans, the sample is placed; the other pan is the reference pan, which is kept empty. Both the pans sit on the top of a heater. Now, the system is switched on where the computer turn on the heaters and it heats the two pans at a specific rate, usually 10°C per minute. The computer makes absolutely sure that the heating rate stays exactly the same throughout the experiment.

As the two pans are heated, the computer will plot the difference in heat output of the two heaters against temperature. That is, the heat absorbed by the polymer against temperature is plotted. As the heating of the polymer continues, there is more heat flow. There is an increase in the heat capacity of the polymer sample. This happens because the polymer goes through the glass transition. Above the glass transition, the polymers have a lot of mobility. When they reach the right temperature, they will have gained enough energy to move into very ordered arrangements, in other terms called crystals. When polymers fall into these crystalline arrangements, they give off heat. There is a drop in the heat flow versus temperature curve. The temperature at the lowest point of the dip is

usually considered to be the polymer's crystallization temperature, or Tc. If the heating continues over its Tc, eventually it'll reach another thermal transition, called melting. When the polymer's melting temperature, or *T*m, is reached, the polymer crystals begin to fall apart, that is they melt. The extra heat flow during melting shows up as a peak on the DSC plot.

Thermogravimetric Analysis (TGA)

Thermogravimetric analysis (TGA) was done using TA Q50 instrument (Figure 4.7). It is a thermal analysis technique used to measure changes in the weight (mass) of a sample as a function of temperature and/or time under a controlled atmosphere. TGA is commonly used to determine polymer degradation temperatures, residual solvent levels, absorbed moisture content, and the amount of inorganic (noncombustible) filler in polymer or composite material compositions. TGA instruments are routinely used in all phases of research, quality control and production operations

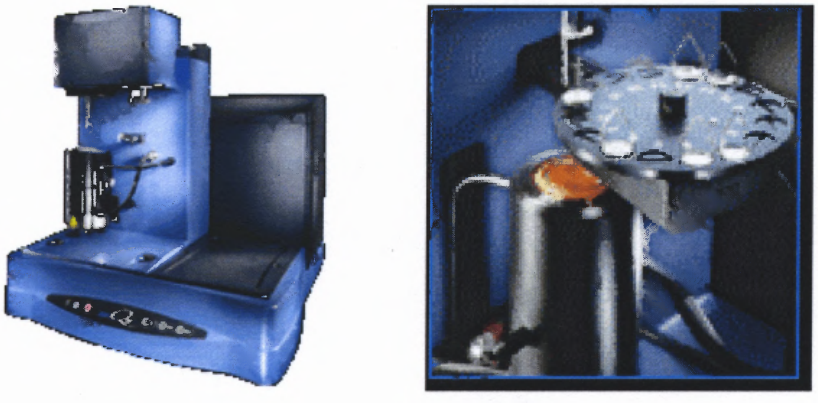

Figure 4.7 TA Q50 Thermogravimetric Analyzer.

A simplified explanation of a TGA sample evaluation may be described as follows. A sample is placed into a tared TGA sample pan, which is attached to a sensitive microbalance assembly. The sample holder portion of the TGA balance assembly is subsequently placed into a high temperature furnace. The balance assembly measures the initial sample weight at room temperature and then continuously monitors changes in sample weight (losses or gains) as heat is applied to the sample. TGA tests may be run in a heating mode at some controlled heating rate, or isothermally. Typical weight loss profiles are analyzed for the amount or percent of weight loss at any given temperature, the amount or percent of noncombusted residue at some final temperature, and the temperatures of various sample degradation processes.

In this experiment TGA is a used for assessing the amount of solvent present in the electrospun mat. The volatilization of residual solvent is typically associated with the initial weight loss process in a TGA heating run. In some cases, absorbed moisture may be liberated over this same temperature range, though. After the initial solvent (or moisture) weight loss process, TGA profiles will typically plateau to some constant weight level until the polymer degradation temperature range is reached. The weight fraction of residual solvent (or moisture) and the onset and maximum rate weight loss degradation temperatures are readily determined by TGA.

4.6.5 Density of Nanofiber Mats

Five samples from various locations of electrospun mats were cut into small pieces of 20mmX12 mm and weighed and their average weight noted. Weight by volume ratio was calculated for all the samples after measuring their thickness.

CHAPTER 5

RESULTS AND DISCUSSIONS (PART 1)

The polymers used for this experiment were $P_{DL}LA$, $85/15P_{DL}LGA$, $50/50P_{DL}LA$, and P_LLA. Least possible concentration was used for all the polymers, as that would yield small diameter nanofibers. The lowest possible concentration required for spinning varied for different polymers. For the entire polymer samples constant parameters for spinning were maintained, the voltage used was 30KV, the distance between the tip and the target was 20cm, a 20guage needle and methylene chloride as solvent was used. Uniform mats of 200mmLX100mmWX0.5mmH were made. These mats were cut into rectangular strips of 100mmX12mmX0.5mm and tested for tensile properties before and after incubation in PBS solution. The values of the stress strain graphs shown are the nearest values to the average values of the five samples tested. The range of the diameter size of the nonwoven mat is determined by measuring the least and highest diameter of the fiber from the SEM image.

5.1 Characterization of $P_{DL}LA$ Nonwoven Mats

The lowest concentration required for $P_{DL}LA$ was 20%. Below 15% concentration, amorphous powder was getting deposited while spinning. The SEM pictures at different magnifications are shown in Figure 5.1 and Figure 5.2. The stress strain curves before and after incubation states are shown in Figure 5.3 and Figure 5.4, respectively.

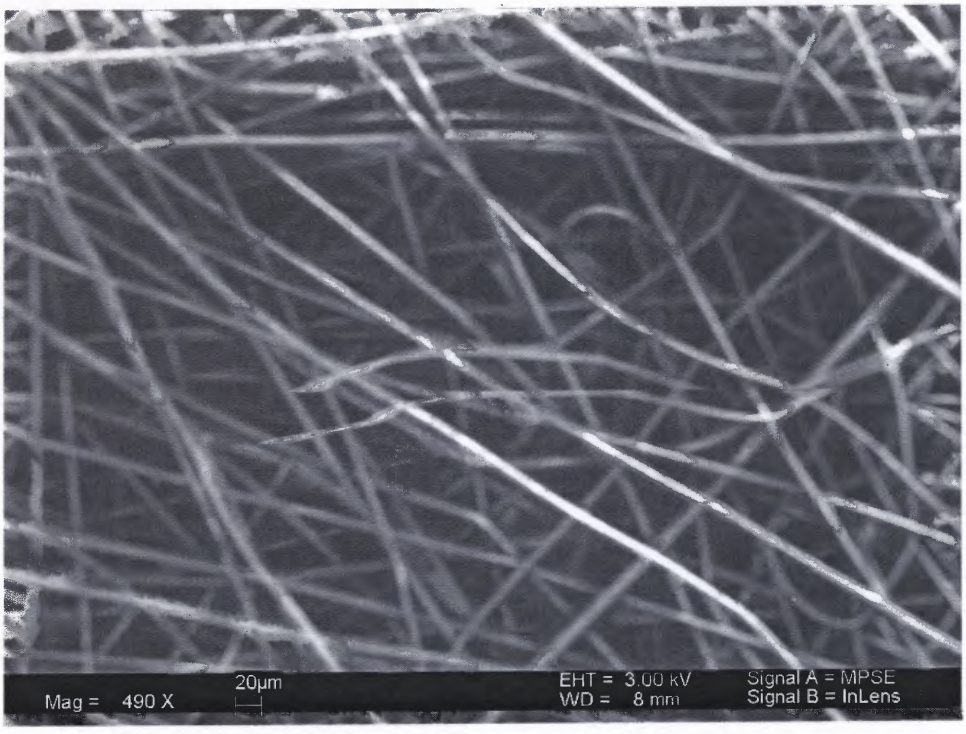

Figure 5.1 SEM picture of $P_{DL}LA$ nonwoven mat at lower magnification.

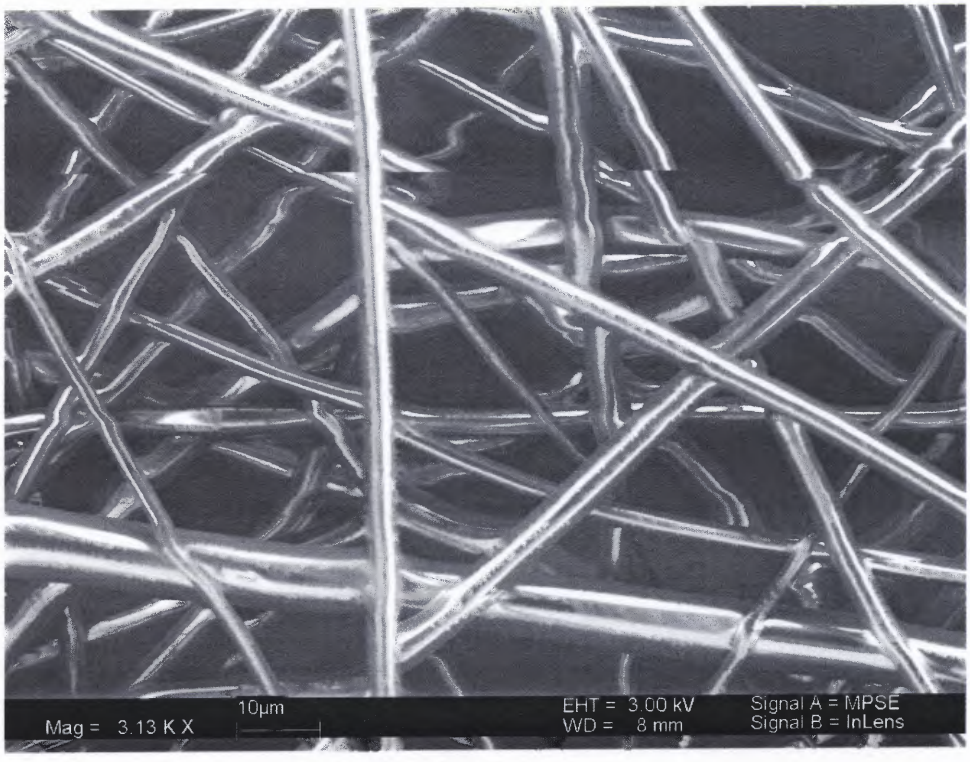

Figure 5.2 SEM picture of $P_{DL}LA$ nonwoven mat at higher magnification.

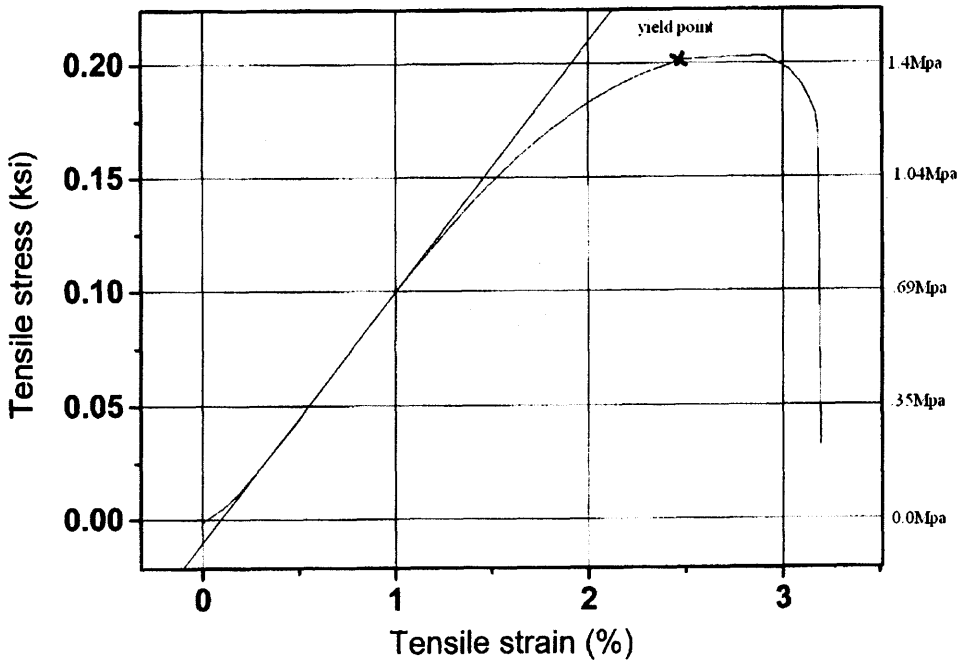

Figure 5.3 Stress-Strain curve of $P_{DL}LA$ nonwoven mat.

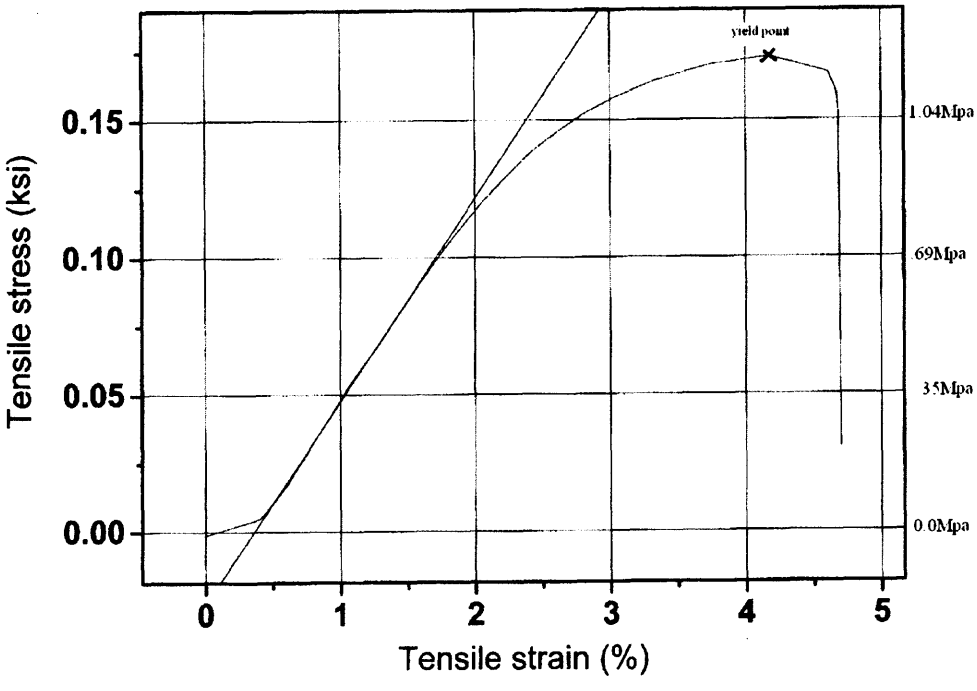

Figure 5.4 Stress-Strain curve of $P_{DL}LA$ nonwoven mat after incubation.

The fibers were very uniform. The range of the fibers produced approximately ranged from 500nm to 2μm. The average weight by volume ratio of the electrospun web is .212 ± .01 gm/ $cm^{3.}$

Table 5.1 Tensile properties of $P_{DL}LA$ Nonwoven Mats

	Yield Strength(Mpa)	Yield Strain(%)	Elasticity(Mpa)
Before Incubation	1.4	2.5	76
After Incubation	1.24	4.2	51

After incubation in the PBS solution at 37 °C for 18 hours the samples lost their shape and they have become stiff. The mechanical behavior has not changed much but there was increase in yield strain observed. Very little decrease in the yield strength is observed. Abrupt break point was observed in both the cases.

5.2 Characterization of 85/15PLGA Nonwoven Mats

The lowest possible concentration required for forming good electrospun mat of 85/15 PLGA was 14%. The SEM pictures of 85/15PLGA at different magnifications are shown in Figure 5.5 and Figure 5.6. The stress strain curves before and after incubation are shown in Figure 5.7 and Figure 5.8, respectively

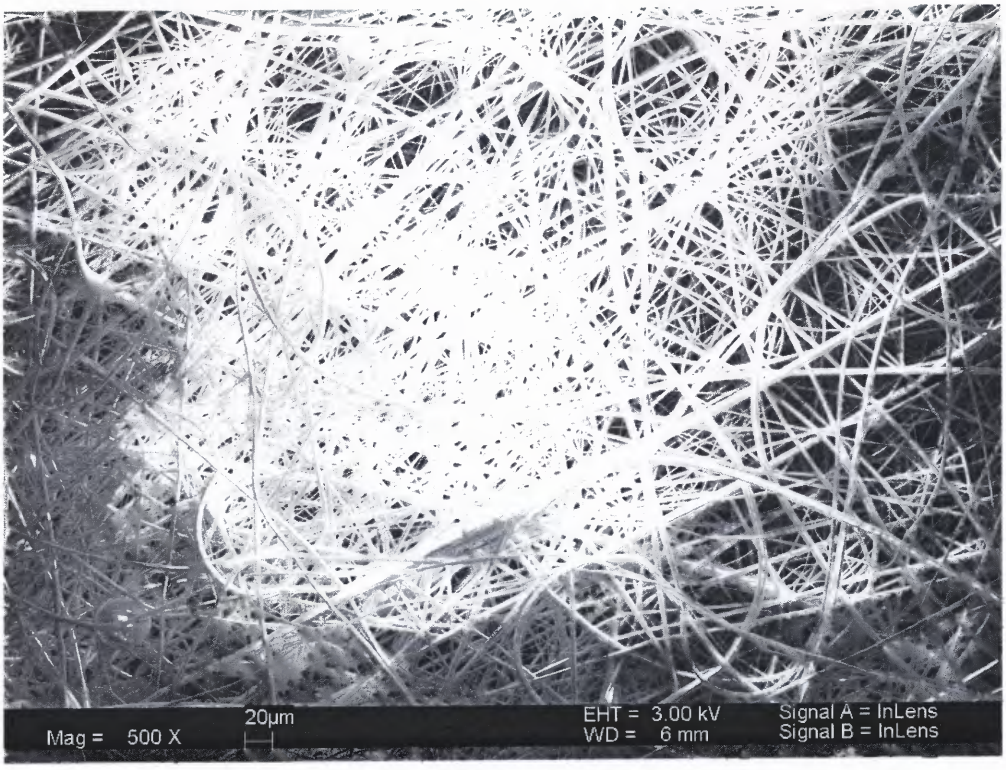

Figure 5.5 SEM picture of 85/15PLGA nonwoven mat at lower magnification.

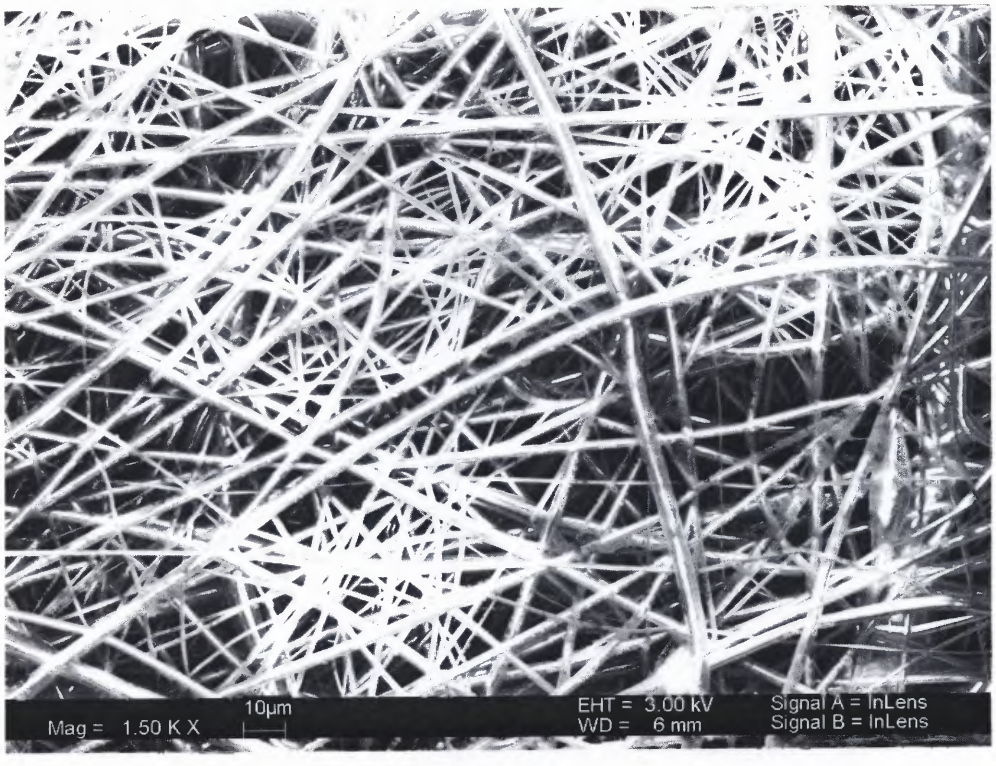

Figure 5.6 SEM picture of 85/15PLGA nonwoven mat at higher magnification.

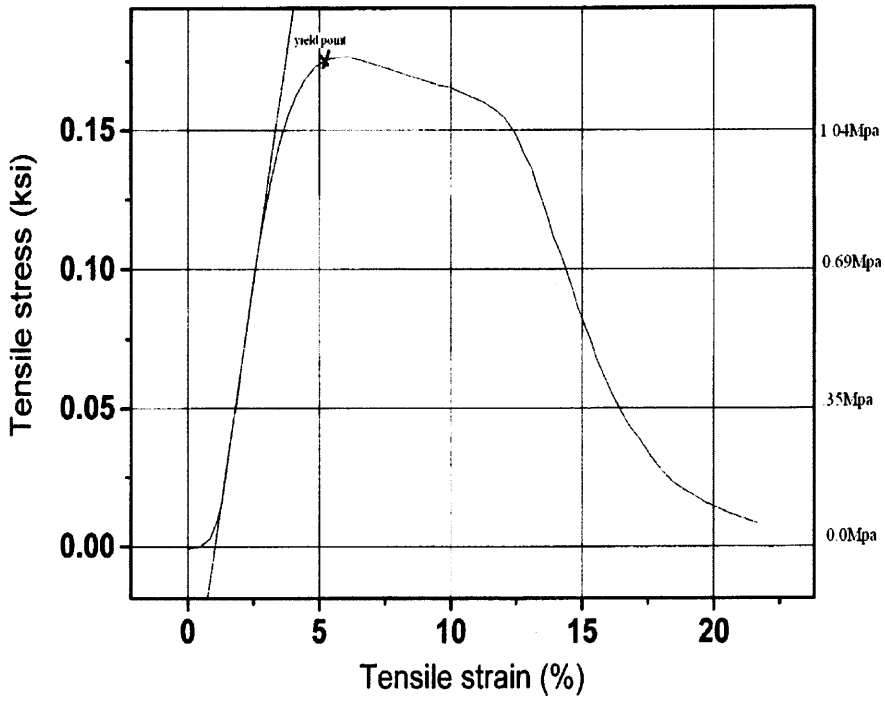

Figure 5.7 Stress-Strain curve of 85/15PLGA nonwoven mat.

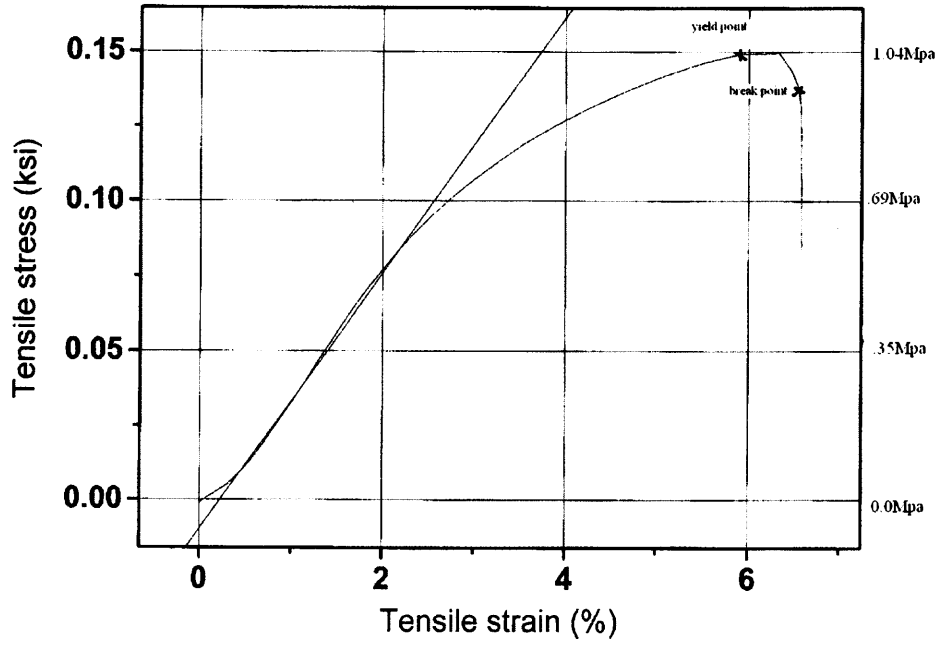

Figure 5.8 Stress-Strain curve of 85/15 PLGA nonwoven mat after incubation.

The diameter of these fibers also approximately ranged from 300nm to 2μm. The fibers were uniform and mostly in the nanoscale. The average weight by volume ratio of the electrospun nonwoven web is .219± .016gm/ cm^3.

Table 5.2 Tensile properties of 85/15 PLGA Nonwoven Mats

	Yield Strength (Mpa)	YieldStrain (%)	Elasticity(Mpa)
Before Incubation	1.2	5.0	45
After Incubation	1.03	5.9	30

After incubation the mechanical behavior of the samples changed .The material lost its shape and has become brittle. An abrupt break point can be seen only in the case of incubated sample. The yield strain has increased and the yield strength has decreased.

5.3 Characterization of 50/50PLGA Nonwoven Mats

The lowest possible concentration required for forming good electrospun mat of 50/50PLGA was 14%. The SEM pictures at different magnifications are shown in Figure 5.9 and Figure 5.10.

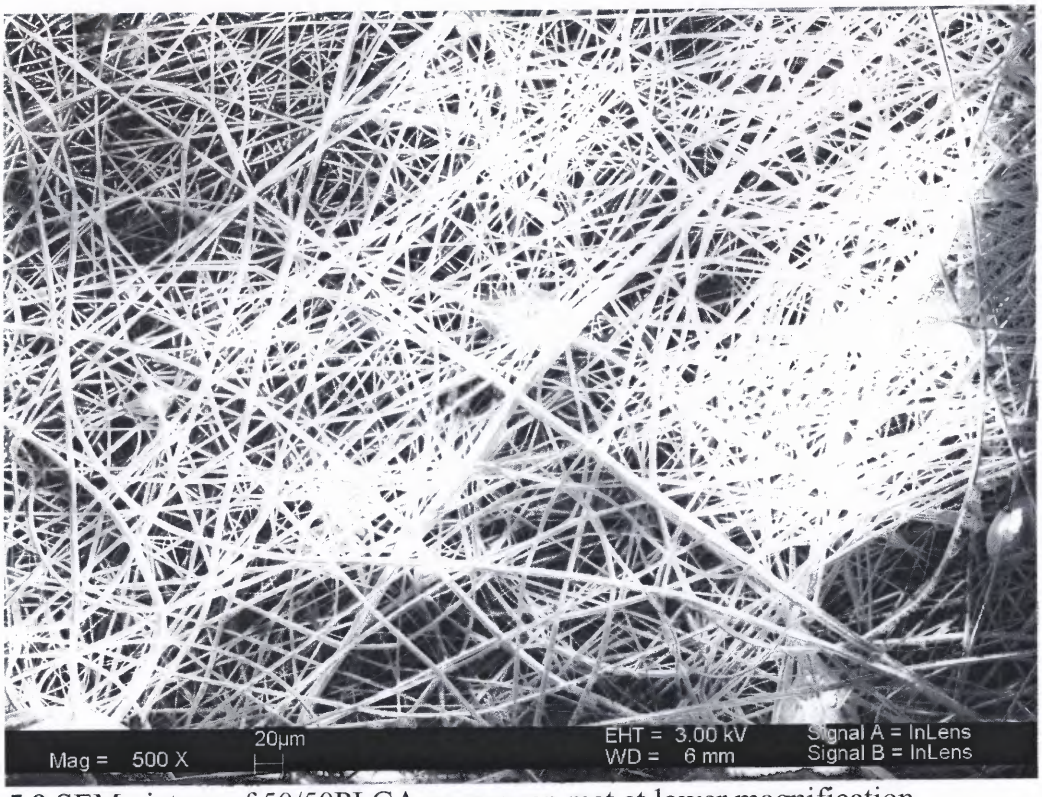

Figure 5.9 SEM picture of 50/50PLGA nonwoven mat at lower magnification

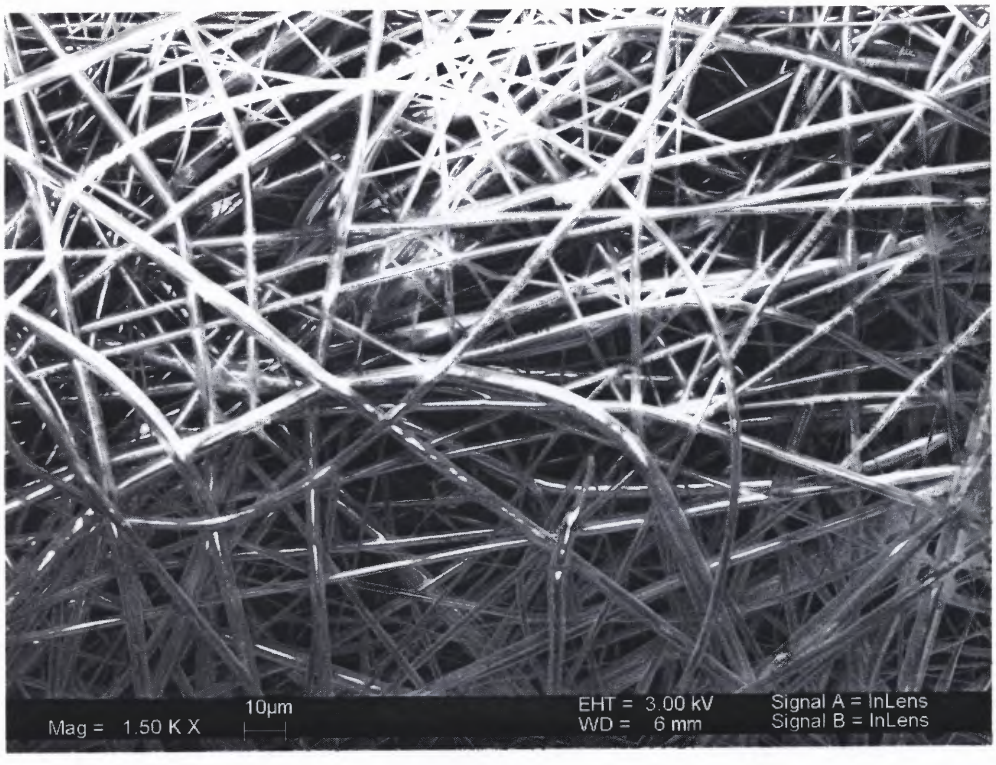

Figure 5.10 SEM picture of 50/50PLGA nonwoven mat at higher magnification.

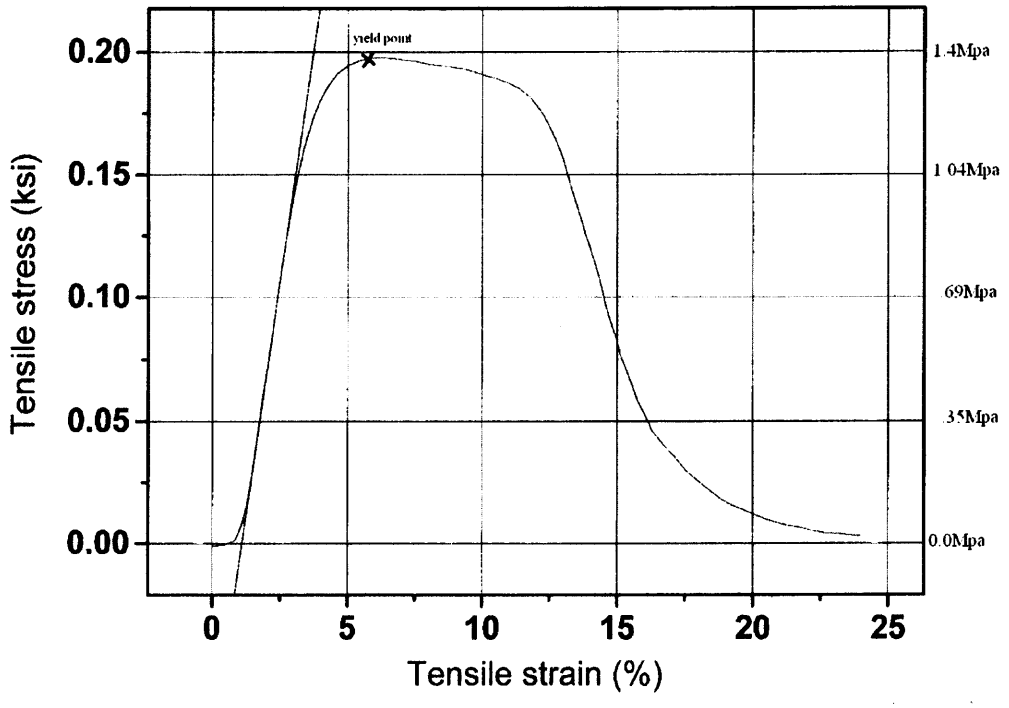

Figure 5.11 Stress-Strain curve of 50/50 PLGA nonwoven mat.

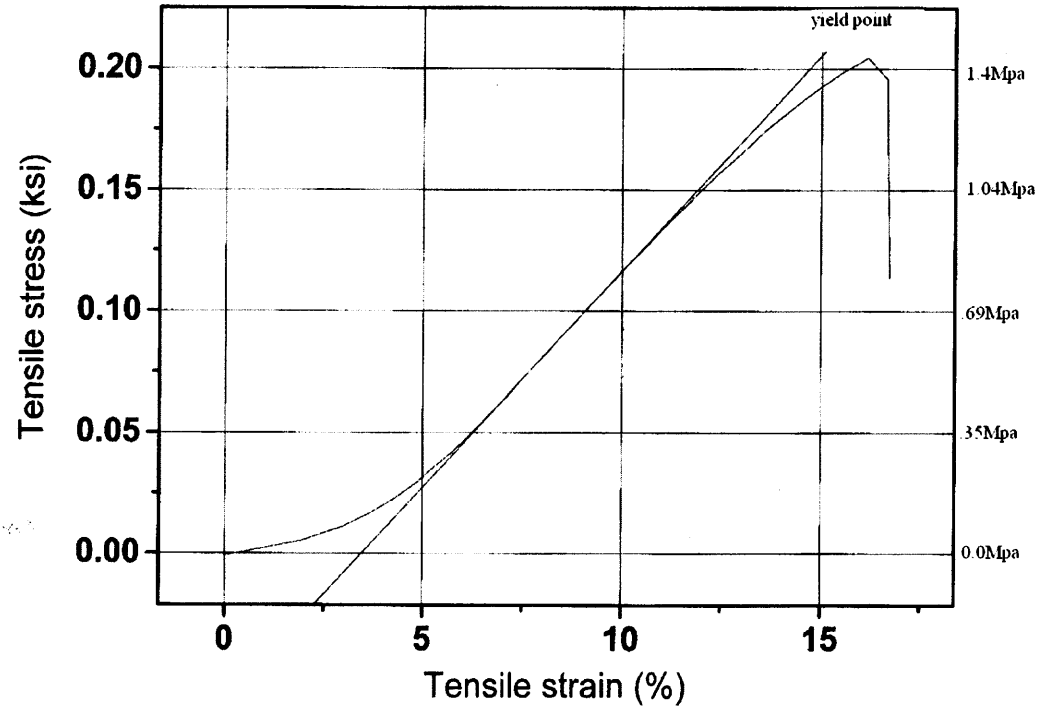

Figure 5.12 Stress-Strain curve of 50/50 PLGA nonwoven mat after incubation.

The fibers produced were uniform and approximately ranged from 300nm to 2μm. The fibers were uniform and mostly in the nanoscale. The average weight(gm)/volume($cm^{3)}$ ratio of the samples is .208 ± .002 gm/ $cm^{3.}$

Table 5.3 Tensile Properties of 50/50PLGA Nonwoven Mats

	Yield Strength(Mpa)	Yield Strain(%)	Elasticity(Mpa)
Before Incubation	1.4	5.4	53
After Incubation	1.4	17	12.4

The graphs of 50/50PLGA samples before and after incubation are shown in Figure 5.11 and Figure 5.12, respectively. The mechanical behavior of the samples changed after incubation. The material lost its shape very badly compared to previous two polymer samples and a very high increase in the yield strain was observed which could be because of the more hydrophilic nature of the polymer. There was not much difference observed in the mechanical behavior.

5.4 Characterization of PLLA Nonwoven Mats

The lowest concentration required for forming a good mat of PLLA was 8%. The SEM pictures of PLLA are shown in Figure 5.13 and Figure 5.14.

Figure 5.13 SEM picture of single PLLA nanofiber

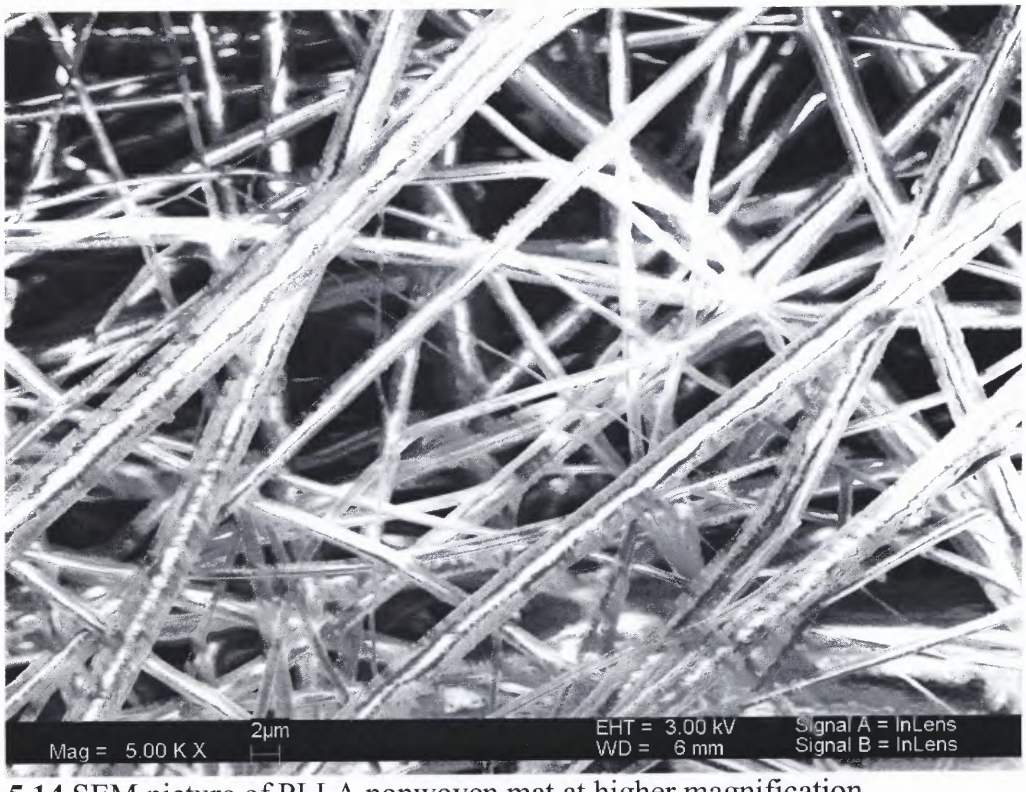

Figure 5.14 SEM picture of PLLA nonwoven mat at higher magnification.

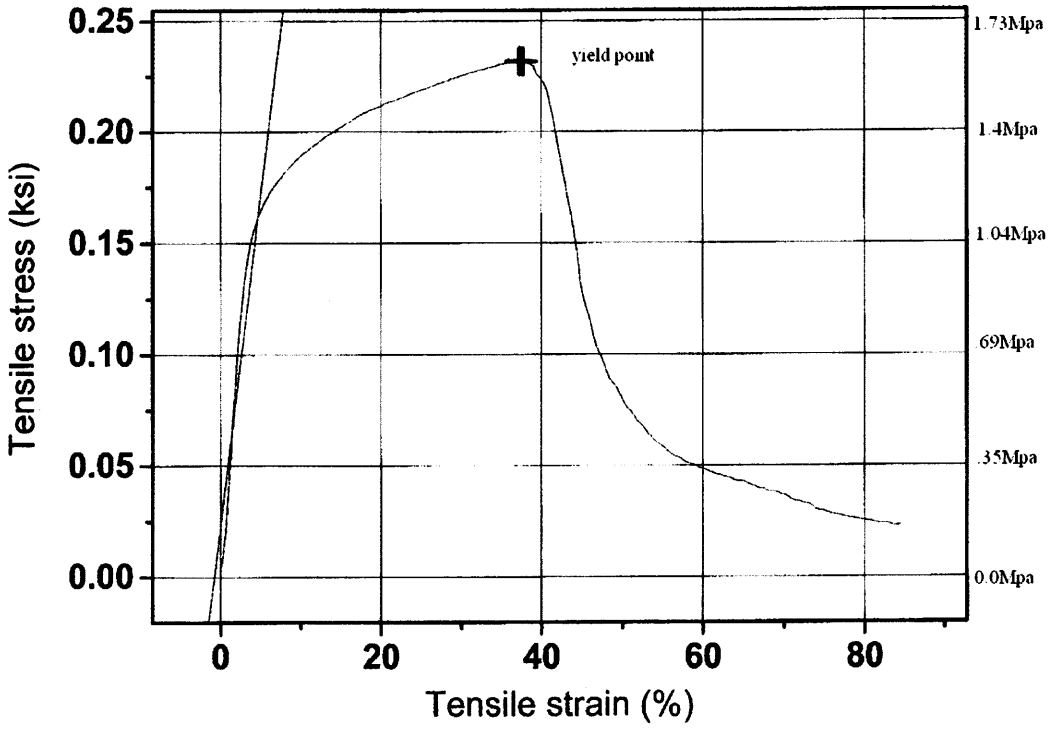

Figure 5.15 Stress-Strain curve of PLLA nonwoven mat.

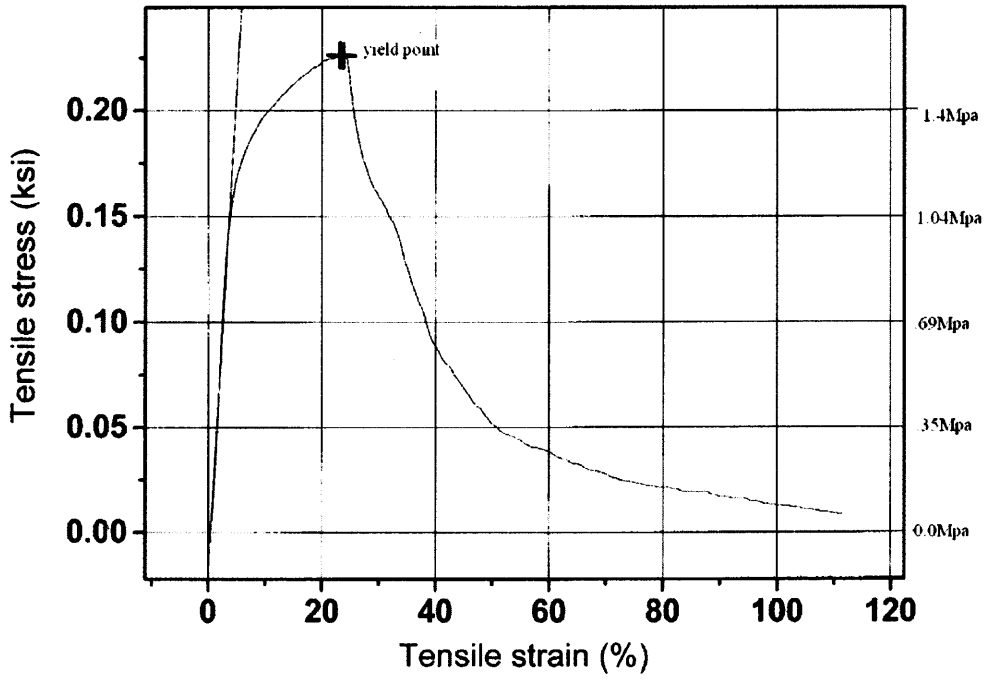

Figure 5.16 Stress-Strain curve of PLLA nonwoven mat after incubation.

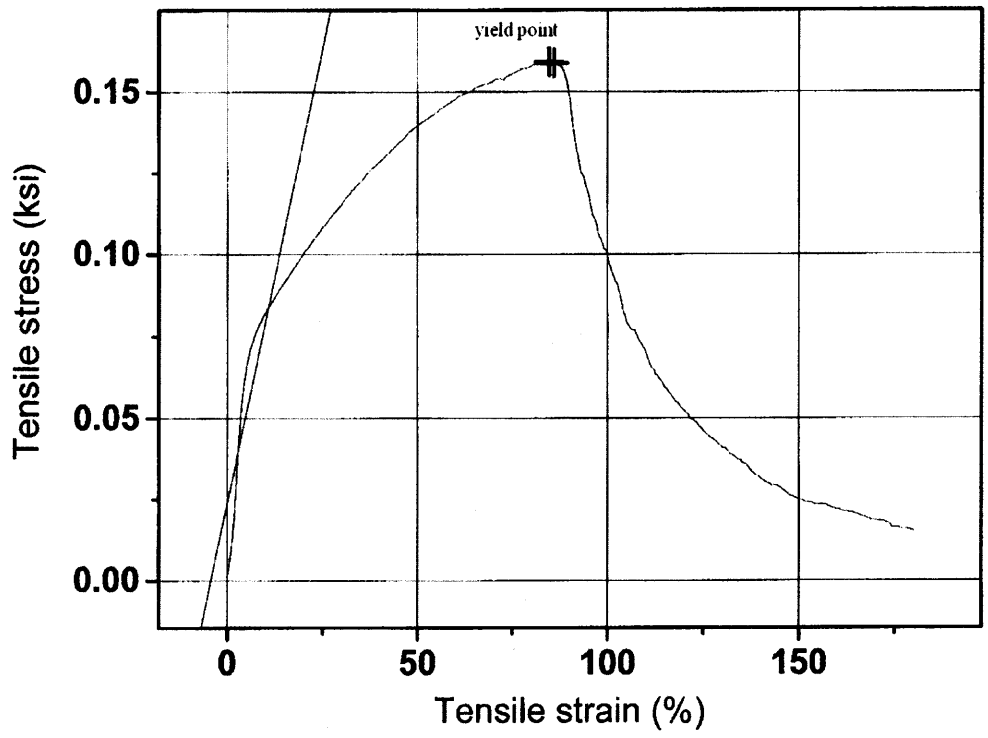

Figure 5.17 Stress-Strain curve of PLLA nonwoven mat tested in perpendicular direction.

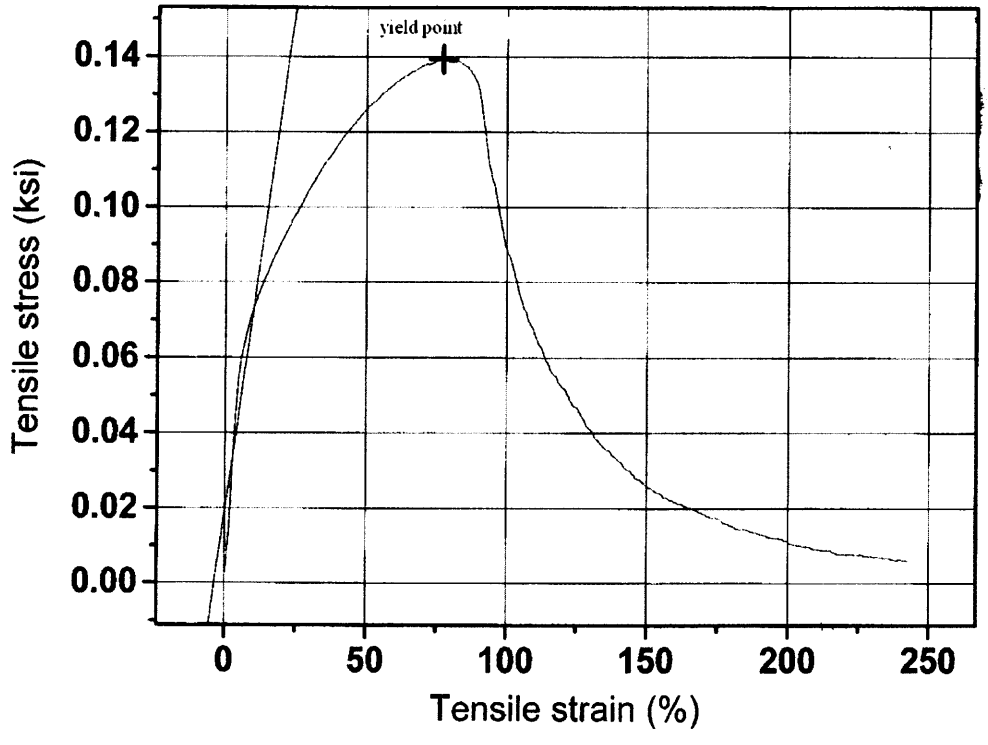

Figure 5.18 Stress-Strain curve of PLLA nonwoven mat tested in perpendicular direction after incubation.

The fibers ranged from 400nm to 4μm. In a PLLA mat the layers of the mats did not stick to each other, it was kind of bushy. The mat of PLLA was very light and soft compared to other lactides, but the mechanical behavior of the PLLA was very interesting. There was necking observed in this case while tensile testing. This mat was also tested for the effect of direction. When tested in the perpendicular direction the yield strength was less and yield strain was more (Figure 5.17 and Figure 5.18). The weight by volume ratio of the electrospun mat was 0.070 ± .005 gm/ cm^3.

Table 5.4 Tensile Properties of PLLA Nonwoven Mats

	Yield Strength(Mpa)	Yield Strain(%)	Elasticity(Mpa)
Before Incubation	1.58	38	20.67
After Incubation	1.55	25	32

Table 5.5 Tensile Properties of PLLA Nonwoven Mats tested in Perpendicular Direction

	Yield Strength(Mpa)	Yield Strain(%)	Elasticity(Mpa)
Before Incubation	1.1	85	4.13
After Incubation	.96	75	3.5

The mat did not lose its shape at all after incubating in PBS solution. There was not much difference observed in the yield strength after incubation but the yield strain has decreased.

CHAPTER 6

CONCLUSIONS (PART I)

The process of electrospinning and mechanical characterization was successfully carried out using poly(lactides). The most important parameters found to control the dimensions of the diameter was the concentration and flow rate. There was no considerable difference observed in morphology between different lactide polymer mats.

All the mats after incubating in PBS solution showed an increase in yield strain and a slight decrease in yield strength. The increase in yield strain in case of 50/50PLGA was very high compared to other lactides used.

There was not much difference observed in the yield strength of different lactide non woven mats but a difference in yield strain existed and increased as crystalinity increased, which implies yield strain is material dependent mostly and yield strength is mat interaction dependent.

The considerable change in the tensile properties of PLLA mat if tested in different direction suggest that there are more fibers aligned in one direction.

The yield strength of PLLA mat, which was expected to be very high, compared to other lactide mats ($P_{DL}LA$, 85/15PLGA and 50/50PLGA) was only slightly higher. But the weight by volume ratio of PLLA mat with same thickness is very less, almost one third of

other lactides used. This suggests that a better way to compare mats would be by density of mats instead of thickness.

CHAPTER 7

RESULTS AND DISCUSSIONS (PART II)

The results of the experiment designed to compare the mechanical behavior of the freshly prepared solution mat and stored solution (around 4 days) mat are shown in this part. The polymer chosen was poly (ϵ-caprolactone) (PCL) and the solvent was methylene chloride. For the entire polymer samples constant parameters for spinning were maintained, the voltage used was 30KV, the distance between the tip and the target was 20cm, a 20guage needle and methylene chloride as solvent was used. Uniform mats of 100mmLX50mmWX0.2mmH were made. These mats were cut into rectangular strips of 50mmX12mmX0.2mm and tested for tensile properties. The values of the stress strain graphs shown are the nearest values to the average values of the five samples tested. The range of the diameter size of the nonwoven mat is determined by measuring the least and highest diameter of the fiber from the SEM image.

7.1 Morphology and Tensile Properties of PCL Nonwoven Mats

The least possible concentration, which would form a good mat, was 10%. The thickness of the mat produced is 0.2mm. The SEM picture of single nanofiber of PCL is shown in Figure 7.1

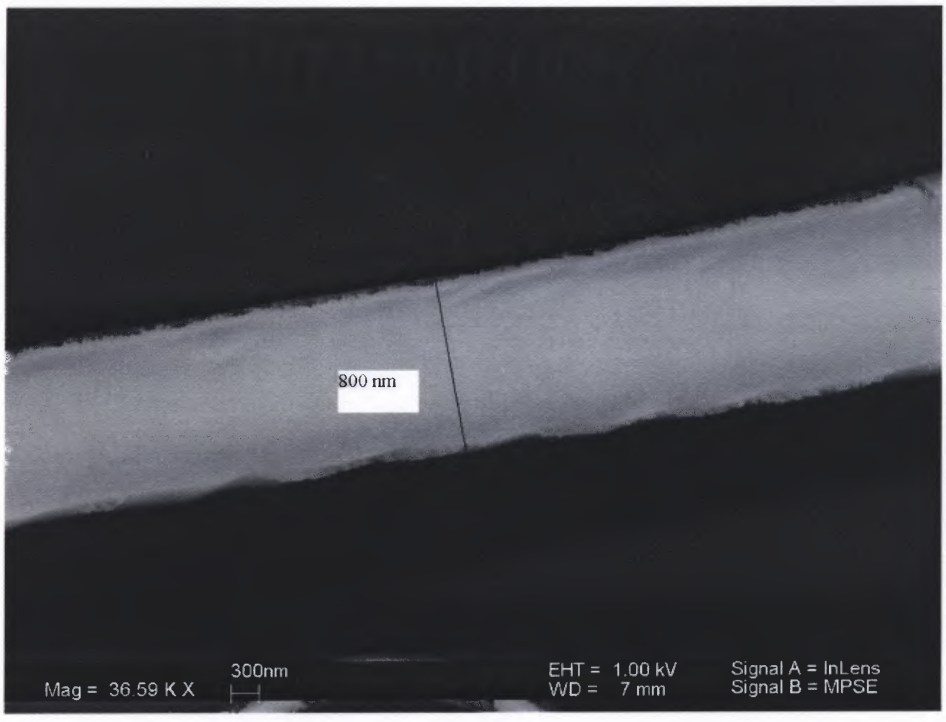

Figure 7.1 SEM picture of single PCL nanofiber.

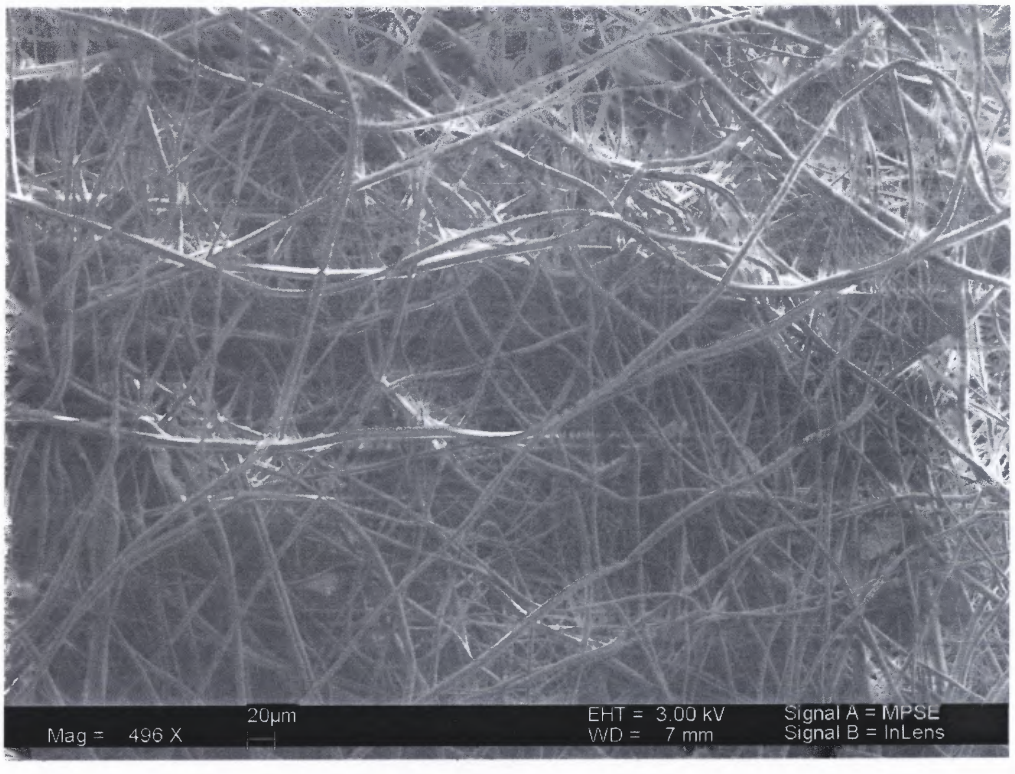

Figure 7.2 SEM picture of 10% PCL fresh solution nonwoven mat.

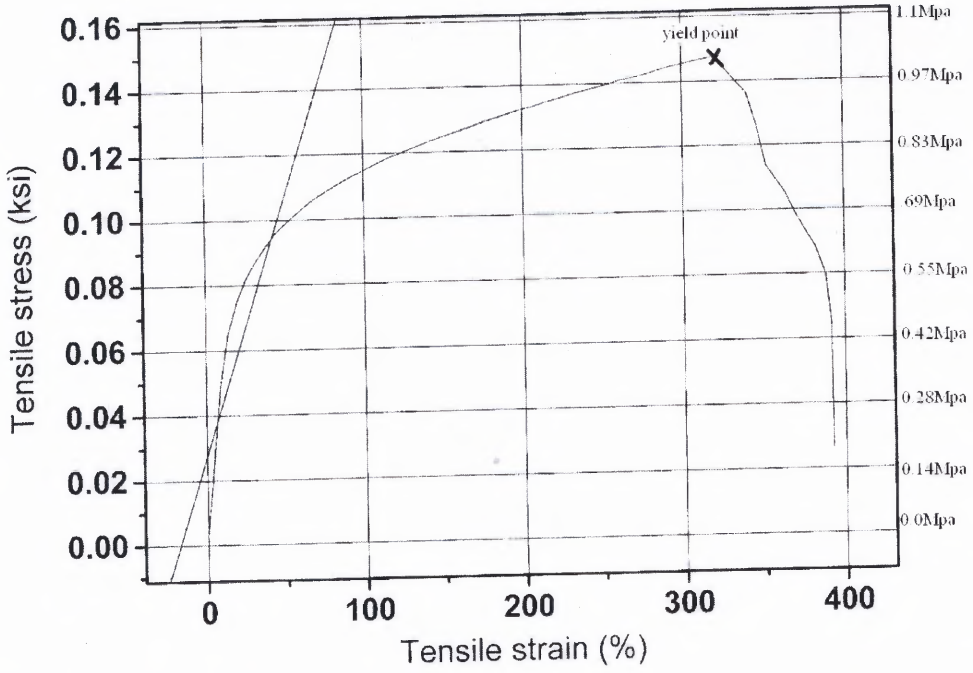

Figure 7.3 Stress Strain curve of 10% PCL fresh solution nonwoven mat.

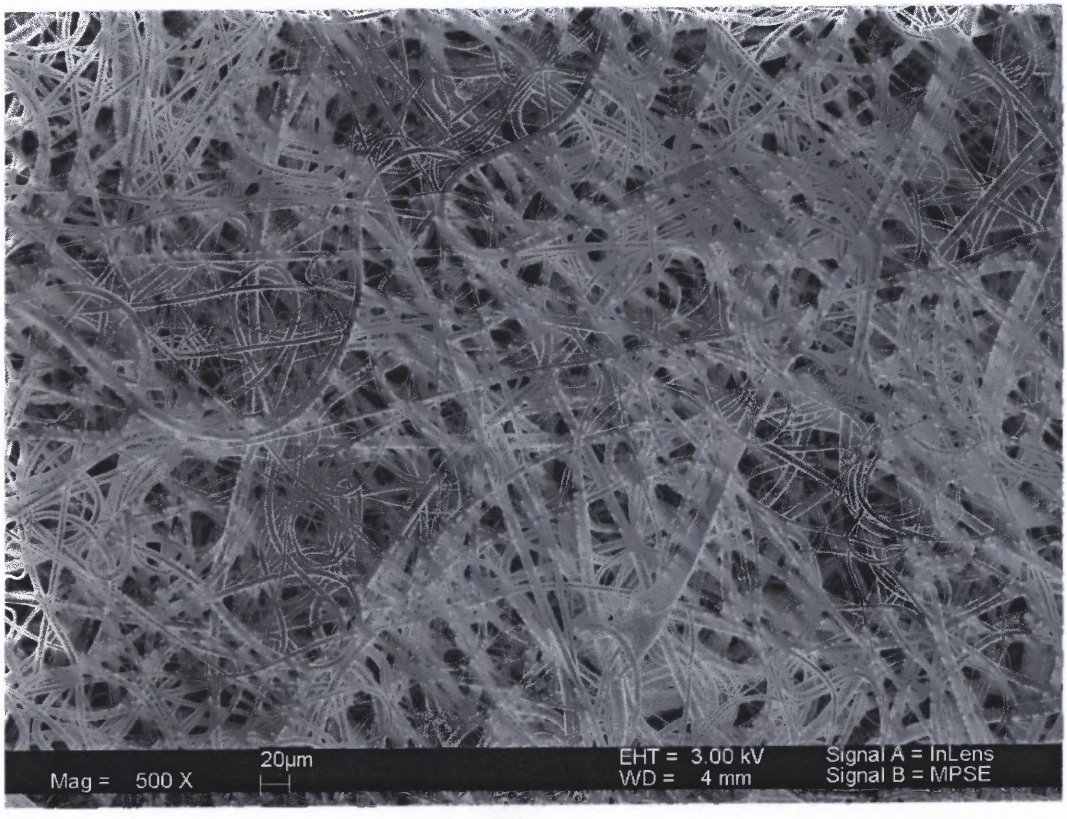

Figure 7.4 SEM picture of 10% PCL stored solution nonwoven mat.

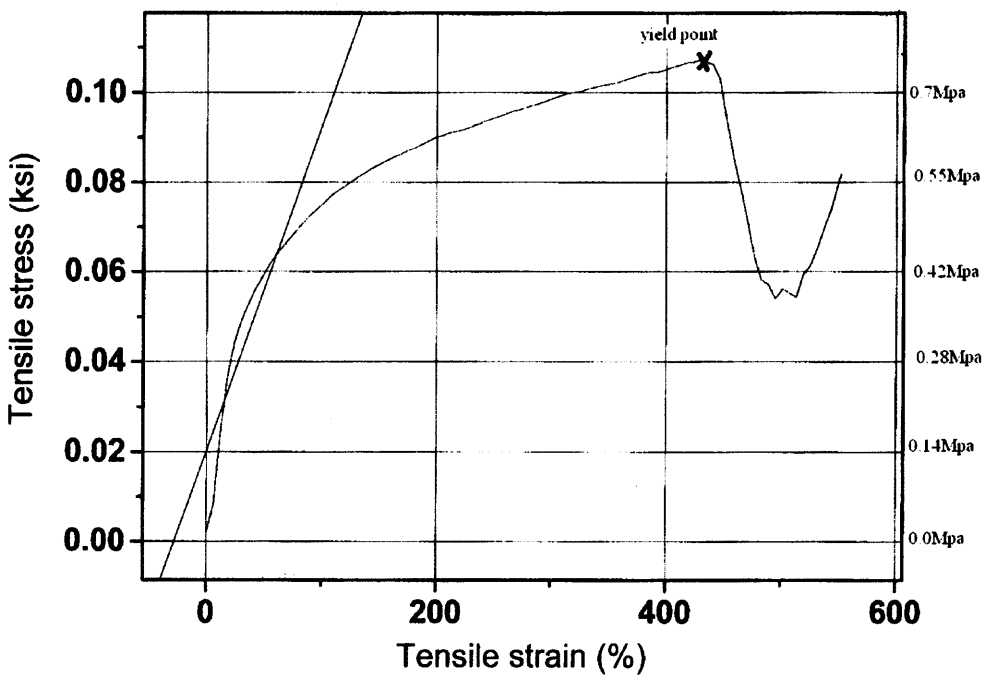

Figure 7.5 Stress Strain curve of 10% PCL stored solution nonwoven mat.

The difference in visual appearance between the stored solution mat and the fresh solution mat can be seen in their SEM pictures and difference in their mechanical behavior can be seen in their stress strain curves.

The SEM picture of 10% fresh solution mat is shown in the Figure 7.2. The fiber diameter approximately ranged from 500nm to 2μm with most of them being in nanoscale. From SEM picture it can be seen that most of the fibers are aligned straight. The weight by volume ratio was .187 ± .012 gm/ cm^3. From the stress strain curve of the mat (Figure 7.3) it can be seen that the mat has broken abruptly. There was no necking behavior observed here.

The SEM picture of 10% stored solution mat is shown in the Figure 7.4. The fiber diameter of this mat also approximately ranged from 400nm to 2μm. From SEM picture it can be seen that the fibers are more curved. The weight by volume ratio of this mat was .172 ± .016gm/ cm^3. From the stress strain curve of the mat (Figure 7.5) it can be seen that the mechanical behavior of this mat is completely different from that of the new solution mat. Here the fibers do not break abruptly and a break point cannot be seen in the curve. There was also a necking behavior observed in this case. Most of vertically aligned fibers in the mat did not break before the maximum limit of the machine gauge length has reached. This kind of behavior is observed when the material in the neck stretches only to a natural draw ratio (which is a function of temperature and specimen processing), beyond which the material in the neck stops stretching and new material at the neck shoulders necks down. The neck then propagates until it spans the full gage length of the specimen, a process called drawing. It occurs when the necking process produces a strengthened microstructure whose breaking load is greater than that needed to induce necking.

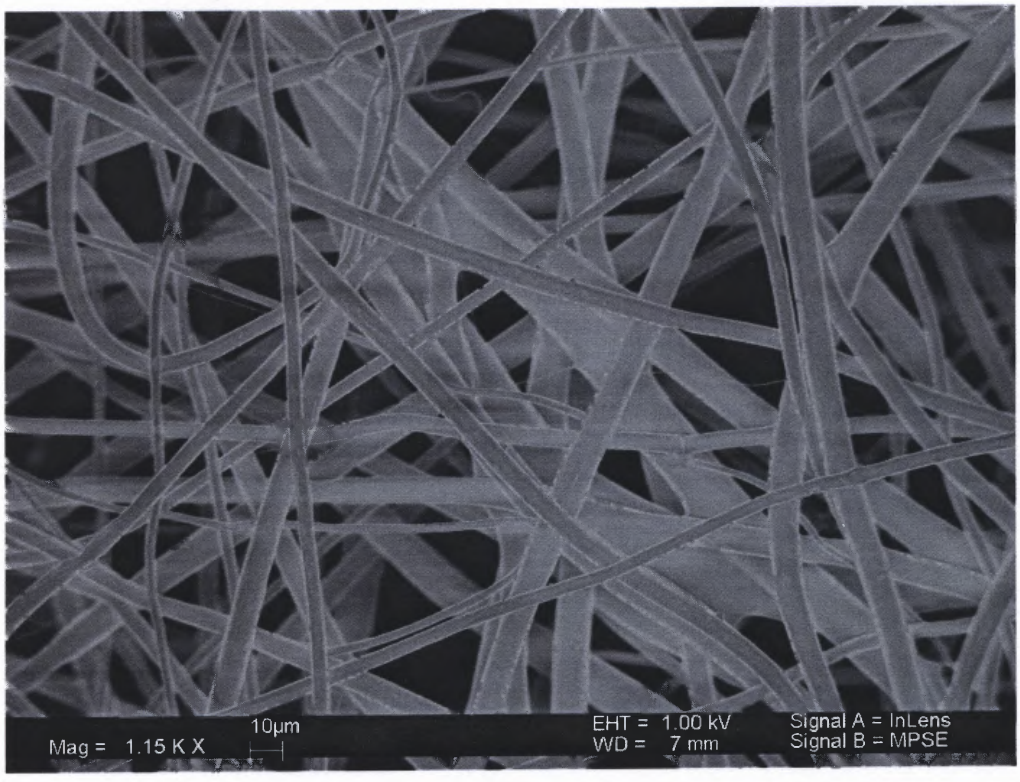

Figure 7.6 SEM picture of 12% PCL fresh solution nonwoven mat.

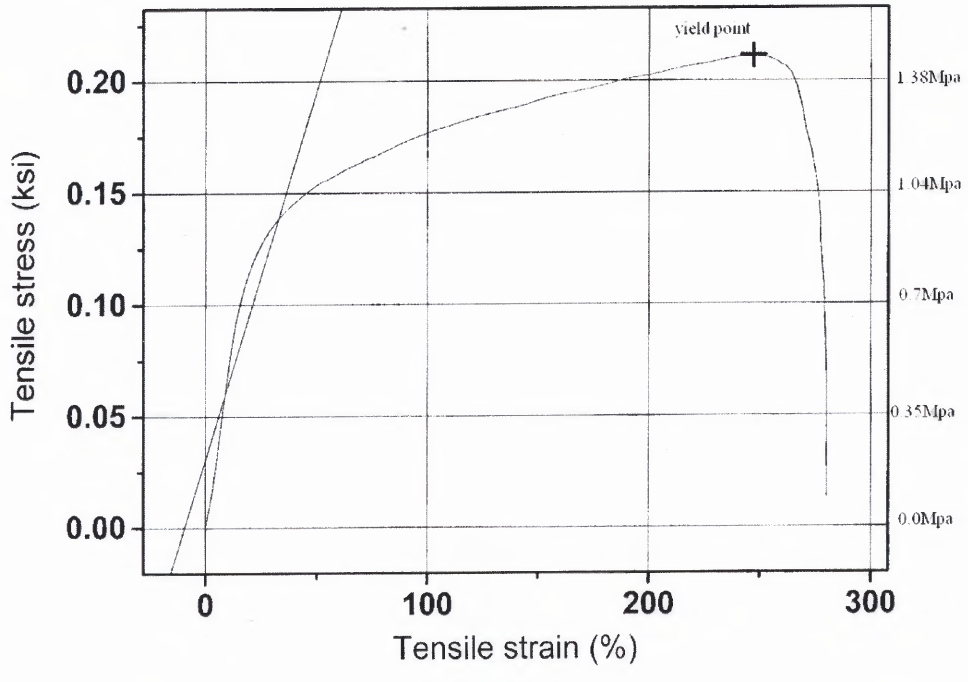

Figure 7.7 Stress Strain curve of 12% PCL fresh solution nonwoven mat.

Figure 7.8 SEM picture of 12% PCL stored solution nonwoven mat.

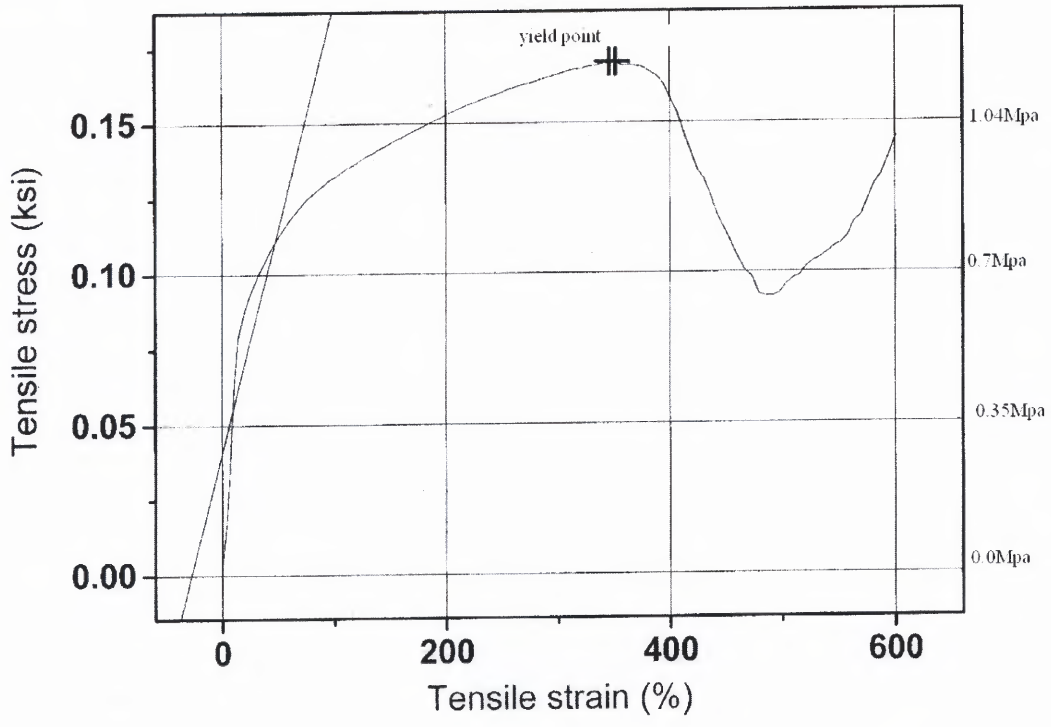

Figure 7.9 Stress Strain curve of 12% PCL stored solution nonwoven mat.

The same study was conducted on higher concentrated solutions and observed similar behavior. The SEM picture and stress strain curves of 12% PCL fresh solution and stored solution mats are shown in the Figure 7.6, Figure 7.7 and Figure 7.8, Figure 7.9, respectively.

Table 7.1 Tensile Properties PCL Electrospun Nonwoven Mat

	Yield Strength (Mpa)	Yield Strain(%)
10% PCL (fresh solution)	1.03	330
10% PCL (stored solution)	0.76	440
12% PCL (fresh solution)	1.45	250
12% PCL (stored solution)	1.17	350

The yield strength of the stored solution mat was observed to be less than the fresh solution mat and the yield strain of the stored solution mat was more than the fresh solution mat. The effect of concentration on both types of solution was also investigated. With the increase in concentration it was observed that the tensile strength increased but the tensile strain was decreased for both old solution mat and new solution mat. Their values are shown in the Table 7.1

The difference in the behavior between the two mats can also be clearly seen in the SEM pictures of the deformed samples after tensile testing. The Figure 7.10 shows the picture of new solution mat and the Figure 7.11 is the picture of old solution mat. The Figure 7.10 shows picture of the fresh solution mat taken at the edge of broken side after it is broken. In case of fresh solution mat very few fibers distantly present can be seen at

the edge. The Figure 7.11 is the picture of the sample after tensile testing at the necking region. It can be seen that fibers are closely aligned in the case of stored solution mat and by the end of test the mat did not break and only vertically aligned fibers were present. From the SEM pictures it can also be predicted that the fiber diameter has decreased after drawing in case of stored solution mat.

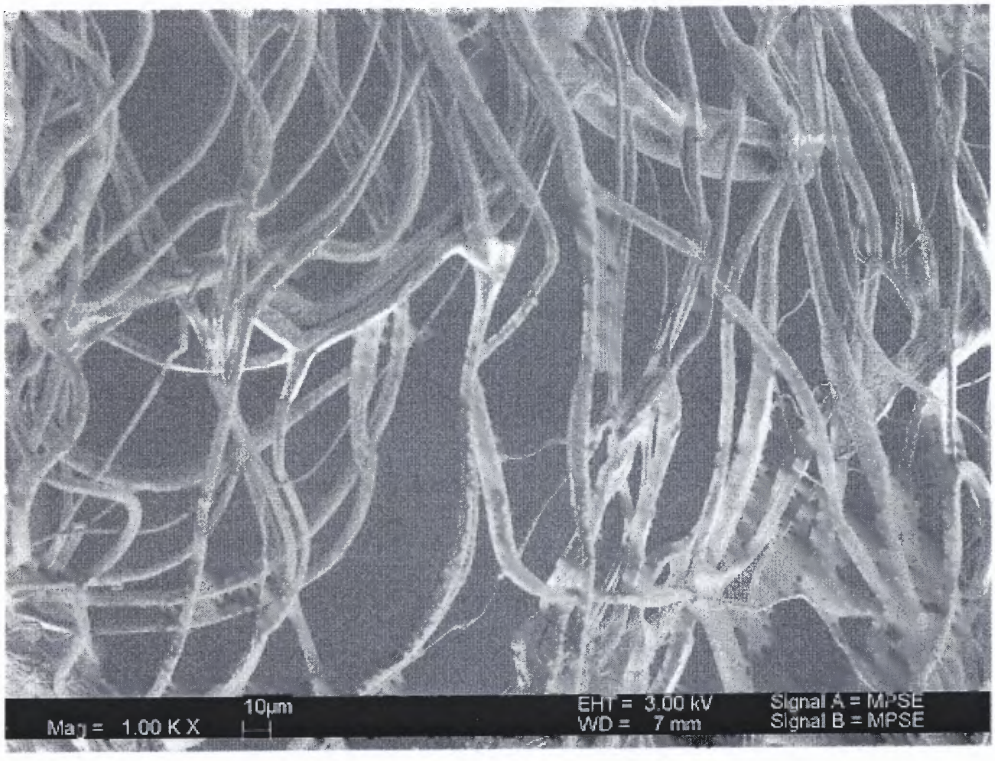

Figure 7.10 SEM picture of 12%PCL new solution mat after tensile testing at broken edge.

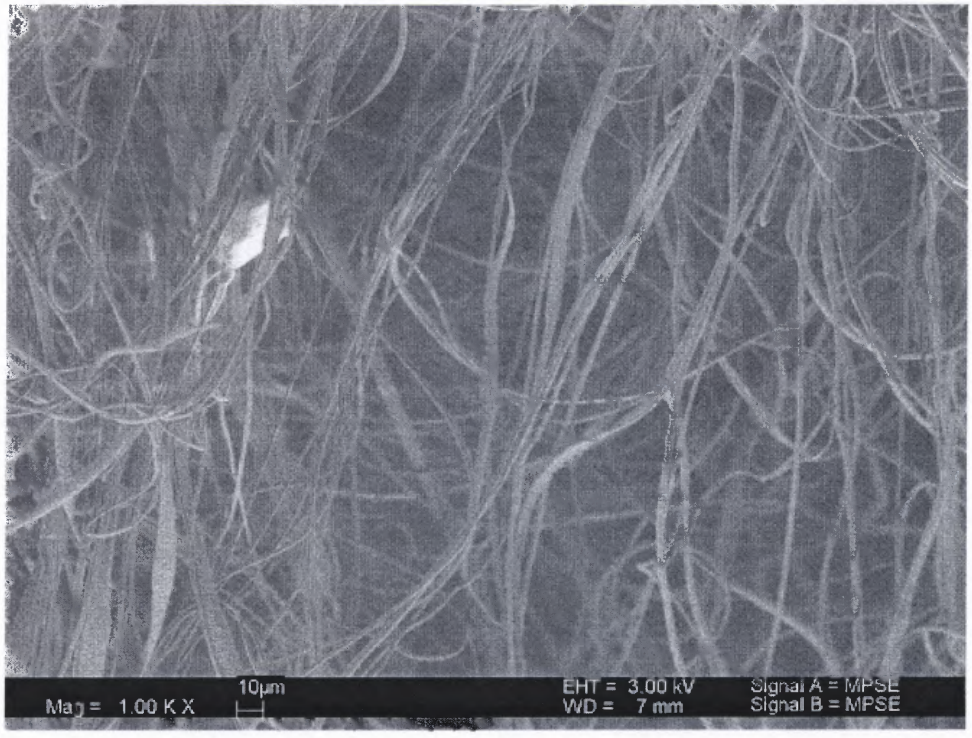

Figure 7.11 SEM picture of 12%PCL old solution mat after tensile testing at the necking region.

7.2 Characterization of Shear Viscosity

In order to understand why exactly they were behaving like this, shear viscosities of the 10 % PCL three days old solution and freshly prepared solutions were studied using the Rheometrics rheometer. The Figure 7.12 is the graph of rheometer reading of the viscosities. The experiment was done at room temperature (22 ° C). Steady shear rates of 20, 50, 100 and 200 were applied for 15, 10, 5 and 5 seconds respectively for a total of 35 seconds.

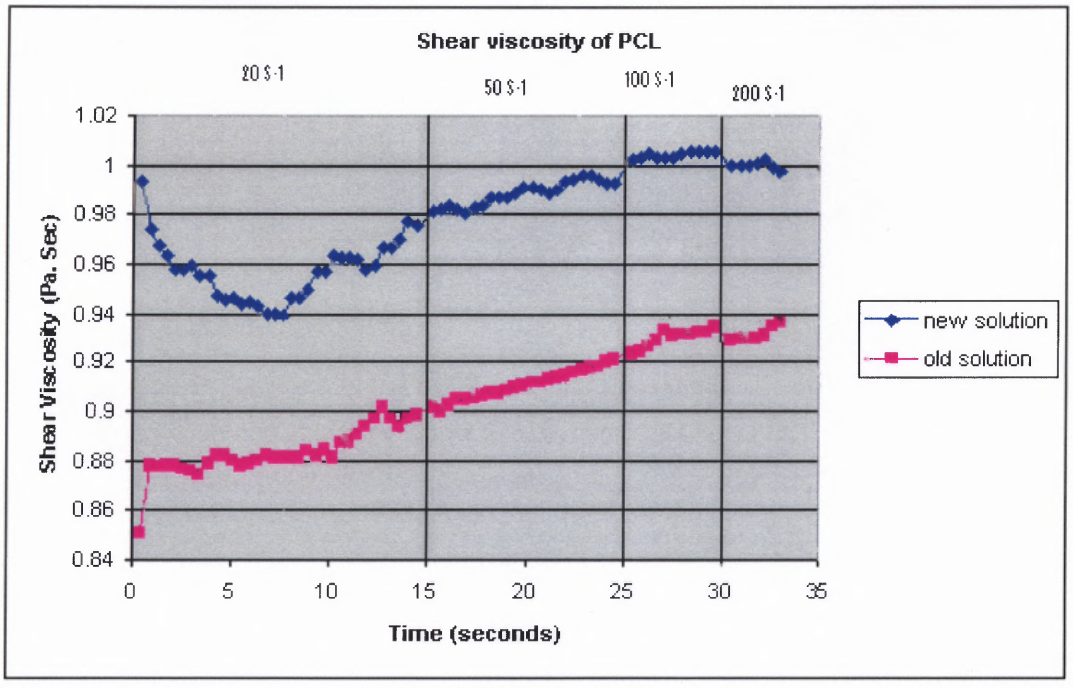

Figure 7.12 Rheometrics Rheometer reading of 10% PCL solution.

From the graph it can be seen that the viscosity of stored solution was less than new solution. In case of new solution, viscosity had decreased initially for some time; this can be predicted to be disentanglement of the molecules. After the disentanglement the viscosity started to increase. Whereas, in the case of stored solution an abrupt increase in the viscosity is found initially and any disentanglement kind of behavior is not observed. From this it is understood that the molecules were already disentangled incase of stored solution. This could be because of long standing of the solution.

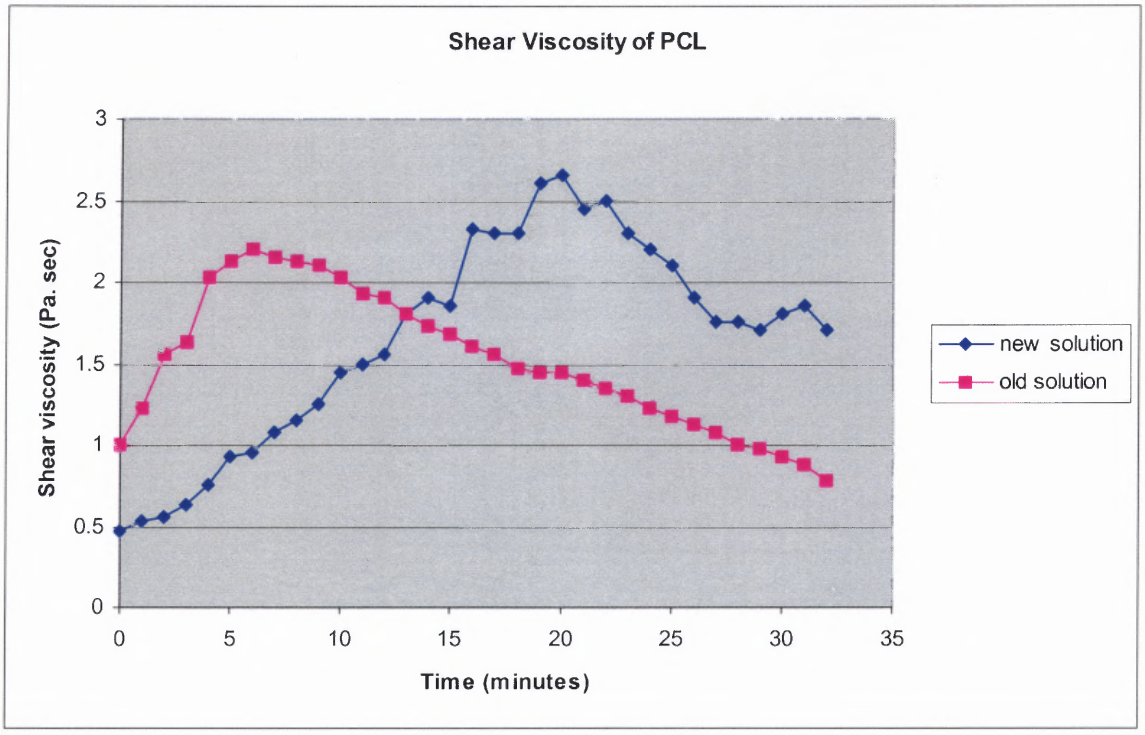

Figure 7.13 Brookfield Viscometer reading of 10% PCL solution at constant shear rate.

In order to further clarify the results the viscosity of stored solution and fresh solution were found using Brookfield viscometer at constant shear rate. The Figure 7.13 is the graph of Brookfield viscometer readings taken at constant shear rate of 38.4 sec^{-1} and at room temperature (18° C). Readings were noted for half an hour at every minute. This experiment also has proved that viscosity of old solution was less then new solution. The viscosity of PCL solution was found to be time dependent at constant shear rate. It has increased initially and then started to decrease. The increase in the viscosity could be because of the entanglement of molecules and the decrease could be because of the disentanglement of the molecules. From the graph it can be seen that the new solution has

taken more time to reach maximum value whereas old solution has reached maximum value very soon. The initial rise in the viscosity was also high in the case of old solution. This also suggests that the molecules were already disentangled in case of old solution. There was lots of oscillating behavior observed in the case of new solution whereas old solution was behaving smoothly.

All these results suggest that the molecular arrangement in the case of stored solution is different from that of fresh solution. As viscosity is a measure of the ease with which molecules move past one another, which depends on the attractive force between the molecules and on structural features which cause neighboring molecules to become entangled, it is expected that the fresh solution molecules were entangled and the stored solution molecules were mostly disentangled leading to different molecular arrangement and mechanical behavior of the electrospun mats.

7.3 Thermal Analysis by DSC

To know if the characteristic properties of electrospun mat have changed from that of original polymer DSC experiment was conducted. All the graphs were plotted for temperature °C (X-axis) against the heat flow, (W/g) (Y-axis). Figure 7.14 shows the DSC curve of fresh solution mat and Figure 7.15 shows the curve of stored solution mat. The glass transition and melting point of original PCL polymer are 66°C and 60°C respectively. The melting point, crystallization and glass transition temperature indicates that the characteristic properties of polymer have not changed after electrospinning with methylene chloride as solvent in both the cases. There was also no difference found in the fresh solution mat and stored solution mat.

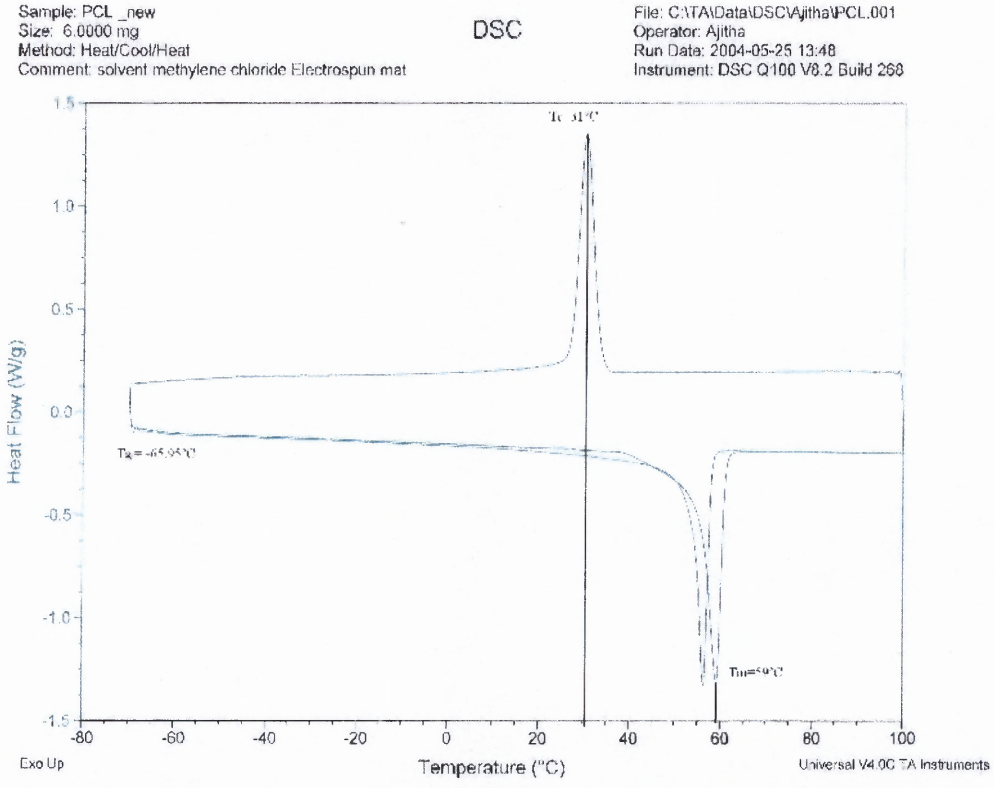

Figure 7.14 DSC thermogram of fresh solution nonwoven mat.

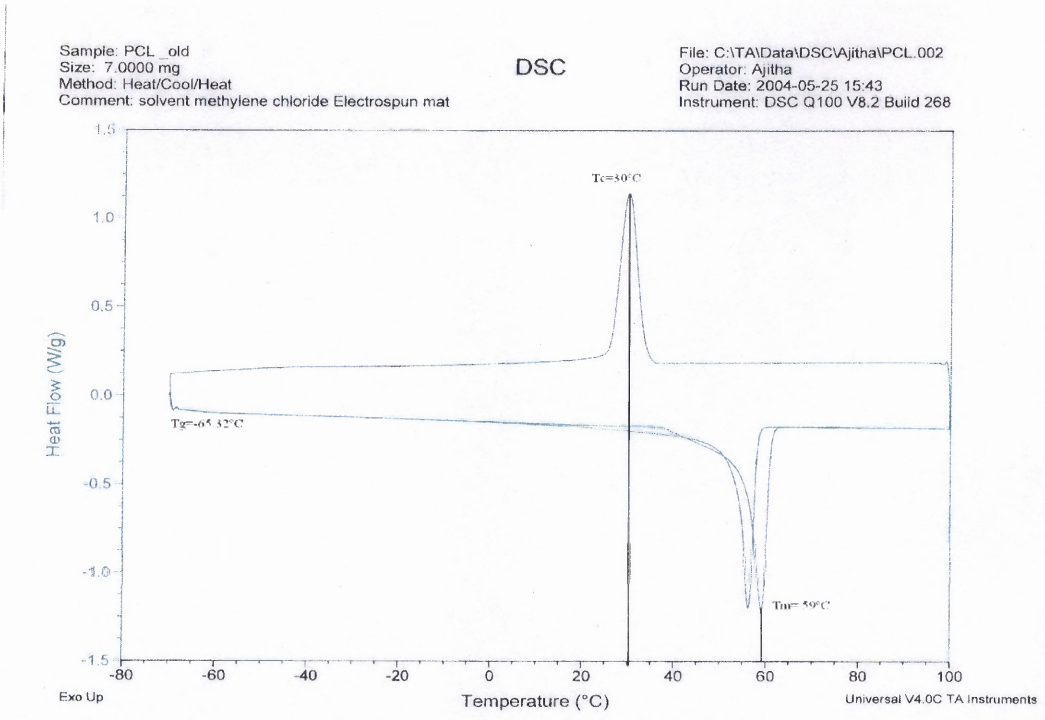

Figure 7.15 DSC thermogram of stored solution nonwoven mat.

7.4 Thermal Analysis by TGA

TGA was run to see if there is any solvent present in the mat after spinning. Figure 7.16 and Figure 7.17 are the thermogram curves of fresh solution mat and stored solution mat. From both the curves it can be seen that there was negligible mass loss (0.14% loss in case of fresh solution mat and .05% in case of stored solution mat). These suggest that there was no solvent present in the electrospun mat.

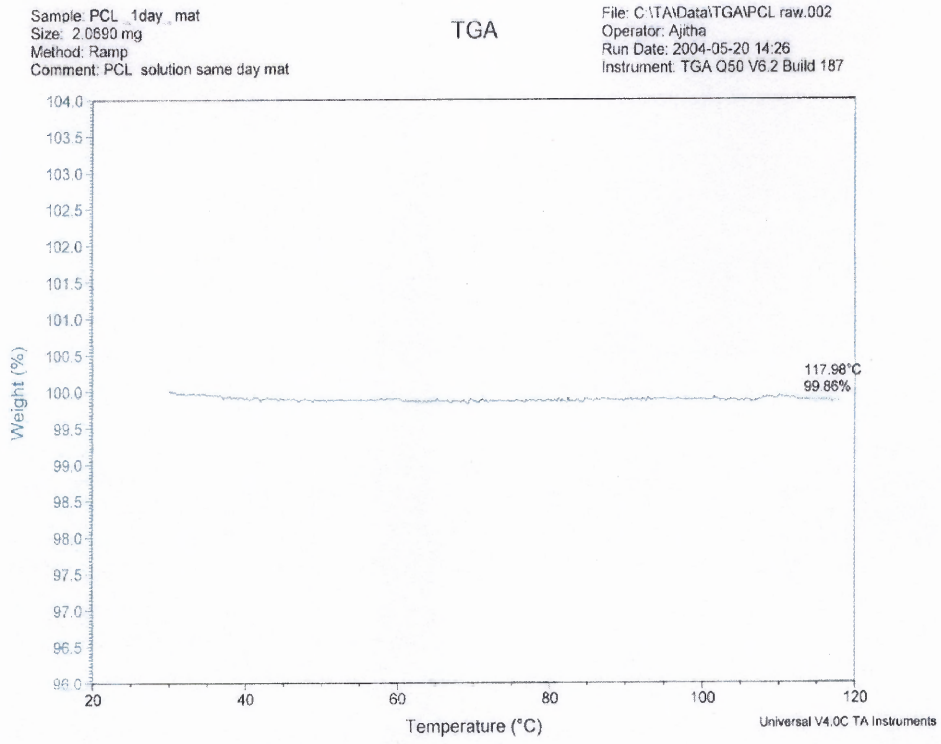

Figure 7.16 TGA thermogram of 10% fresh solution nonwoven mat.

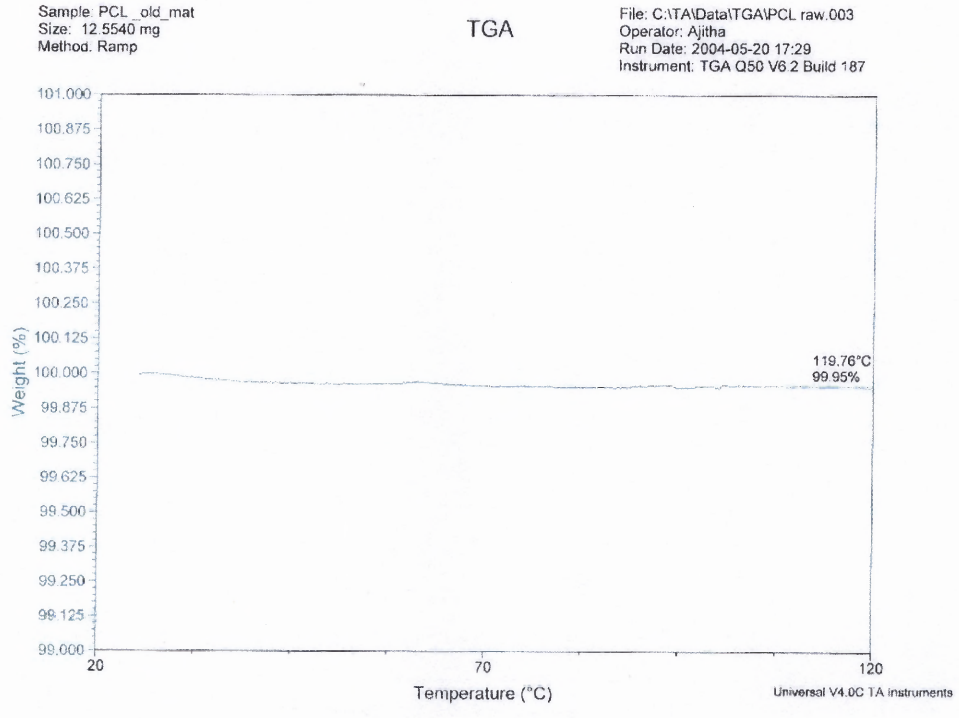

Figure 7.17 TGA thermogram of 10% stored solution nonwoven mat.

CHAPTER 8

CONCLUSIONS (PART II)

The differences in the fresh solution mat and stored solution mat suggest that the aging of the solution affects the properties of electrospun nonwoven mats. Hence, care should be taken while comparing two different mats or comparing any of their applications for example if culturing cells in tissue engineering that consistency in not only other parameters but the age of the solution should also be considered as a critical factor for making mat.

The effect of increase in concentration of solution on the electrospun mat was increase in the yield strength and decrease in the yield strain. This could be because of higher viscosity, which would lead to more molecular entanglements.

The viscosity study of the PCL solution using Brookfield viscometer was complex to understand because the viscosity increased and then decreased at constant shear rate suggesting entanglement and disentanglement respectively. Its viscosity was time dependent. But it was clear enough to understand the differences between fresh solution and stored solution.

The reduction in the strength of the stored solution mat could be because of decrease in viscosity of the solution but the change in mechanical behavior of stored solution mat

from that of fresh solution mat could be because of different arrangement of the molecules.

The shear viscosity behavior undergone by the solution during electrospinning can be related to the behavior seen in the measurement by Rheometrics rheometer as during electrospinning in a very short time the whole process of fluid ejecting out from the syringe needle takes place.

This investigation would definelty contribute towards the further research in the field of electrospinning.

CHAPTER 9

DRAWBACKS

The major drawbacks of this study were:

- Distribution of the diameter size in the nonwoven mats was not being found; only the range could be found by measuring the maximum and minimum diameter from the SEM pictures.

- The mechanical properties of the mat can be further improved with better electrospinning set up, which can form more aligned fibers.

CHAPTER 10

RECOMMENDATIONS

- The behavior observed in the case of PCL electrospun mats could be modeled and can be further investigated and applied on other polymers electrospun mats to know if this kind of behavior does exist or not.

- Cells could be cultured on both types of mats studied in Part II and differences can be investigated.

- The Part II of the thesis could be studied in biorelevant conditions.

- To understand more about the changed properties from fresh solution mat to stored solution mat the molecular arrangement of both the solution mats need to be precisely studied with a suitable instrument.

- So far, no report has been found in the open literature regarding measurement of the mechanical properties of single polymer nanofibers. The biggest challenge in the mechanical characterization is how to isolate a single nanofiber and then how to grip it into a sufficiently small load scale tester.

- A study needs to be conducted to investigate how the diameter and distribution of diameter is affecting the mechanical properties of the mat.

APPENDIX

SAFETY PROCEDURE FOR THE ELECTROSPINNING SET UP

The process of electrospinning involves usage of highly toxic and corrosive chemicals, as well as very high voltage equipment. The person using this equipment should practice extreme measures for their safety. A list of procedures for chemical and electrical safety has been listed below. All persons using this equipment/process should follow these safety measures.

A.1 Chemical Safety

- Always wear eye protection, hand protection and protective clothing.
- Handle the chemicals with care and store them at proper places.
- Make sure the solution is prepared inside the hood and the fumes emerging from the chemicals should be properly ventilated.
- Clean beakers and bottles should be used for transferring of chemicals and preparing of solution.
- Close the bottles of methylene chloride immediately after use and also close the glass lid of the bottle containing the prepared solution.
- The polymer chips added to the solution to dissolve can be assisted using a magnetic stirrer and an external source for stirring.
- Dispose of all contaminated materials properly.
- Get medical help immediately if someone is overexposed to chemicals.

2. Electrical Safety

- The electrospinning system uses electrical power for its operation. Any of these smaller pieces of equipment may produce a potentially damaging or lethal shock or serve to ignite flammable materials. Although such shocks and fires may result from defective equipment, most often they may result from the unsafe practices of the user.
- Make sure the high voltage power supply is grounded
- Turn the system down when the polymer level is near the ending stage

REFERENCES

1. Fibers, [Document posted on the Website of Department of polymer Science, University of Southern Mississippi] Retrieved on December 2003 from the World Wide Web. http://www.psrc.usm.edu/macrog/fiber.htm

2. Materials Science and Engineering 554, Nonwovens Science and Technology. [Document posted on Web site of University of Tennessee]. Retrieved on March, 2004 from the World Wide Web. http://www.engr.utk.edu/mse/pages/Textiles/polyester/polyester.html

3. J. M. Deitzel, J. Kleinmeyer, D. Harris and N. C. Beck Tan (2001). The effect of processing variables on the morphology of electrospun nanofibers and textiles. Polymer, Volume 42(1), 261-272

4. Baumgarten PK. (1971) Electrostatic Spinning of Acrylic Microfibers. Journal of Colloid and Interface Science, Vol. 36(1), 71-79

5. Larrondo L, Manley RS.(1981) Journal of Polymer Science: Polymer Physics Edition, 19, 909-20

6. Formhals A, US Patent (1934), 1,975,504

7. Zheng-Ming Huang, Y. -Z. Zhang, M. Kotaki and S. Ramakrishna (2003). A review on polymer nanofibers by electrospinning and their applications in nanocomposites; Composites Science and Technology, Volume 63(15), 2223-2253

8. K.Jayaraman, M.Kotaki, Y.Z.Zhang and S.Ramakrishna (2003) J Nanoscience Nanotechnolgy.

9. Zheng-Ming Huang, Y.Z. Zhang, M. Kotaki, S. Ramakrishna(2003). A review on polymer nanofibers by electrospinning and their applications in nanocomposites; Composites Science and Technology 63, 2223–2253.

10. Rayleigh, F. R. S., Phil., Mag. (1882) 44, p.184.

11. Zeleny, J., Physical Review, (1914) 3, p. 69.

12. Vonnegut, B., and Neubauer, R.L., Journal of Colloid Science (1952) 7, p. 616.

13. Watchel, R.E., and Lamer, V.K., Journal of Colloid Science (1962) 17, p. 531.

14. Taylor GI. Electrically Driven Jets. Proceedings of the Royal Society of London Series(1969) A Mathematical and Physical Sciences. Vol. 313, 453-475

15. Formhals, A., U.S. Patent,(1934) 1,975,504.

16. Gladding, E.K., U.S Patent,(1939) 2,168,027.

17. Simons H.L., U.S Patent,(1966) 3,280,229.

18. Bornat, A., U.S Patent, (1982) 4,323,525.

19. Baumgarten PK(1971). Electrostatic Spinning of Acrylic Microfibers; Journal of Colloid and Interface Science, Vol. 36(1), 71-79

20. Larrondo, L., and Manley, R.ST.J. (1981) Journal of polymer physics Edition, p.909.

21. Kim J-S, Reneker DH.(1999) Mechanical Properties of Composites Using Ultrafine Electrospun Fibers. Polymer Science, 39(5) p. 849-854.

22. Doshi J, Reneker DH.(1995). Electrospinning Process and Applications of Electrospun Fibers; Journal of Electrostatics,35, 151-160

23. Srinivasan G, Reneker DH.(1995). Structure and Morphology of Small diameter Electrospun Aramid fibers; Polymer international,36,195-201

24. Reneker DH, Chun I.(1996) Nanometre diameter fibers of polymer, produced by Electrospinning; Nanotechnology, 7, 216-223

25. Fang X, Reneker DH.(1997).DNA fibers by electrospinning; Journal of Macromolecular Science- Physics, B36 (2), 169-173

26. Fong H(1999). The study of electrospinning and the physical properties of electrospun nanofibers. Doctoral Dissertation. University of Akron.

27. Mohan, Abhay(2002). Formation and Characterization of Electrospun Nonwoven Webs. Thesis submitted in North Carolina State University

28. Schreuder-Gibson, H.L, Gibson, P(2002). Transport Properties of Electrospun Nonwoven Membranes; International Nonwovens Journal, 21-26.

29. Gregory C. Rutledge. Polymer Science and engineering, Statistical Thermodynamics, Molecular Simulation [Document posted on website of Massachusetts Institute of Technology] www.mit.edu/electrospinning.small.jpg

30. Doshi J, Reneker DH(1995). Electrospinning process and applications of electrospun fibers. J Electrostatics, 35(2-3), 151–60.

31. Atala, Mooeny et. al.(1997) Synthetic Biodegradable Polymer Scaffolds. Boston, MA: Birkhauser.

32. R. P. Lanza, R. Langer, W. L. Chick Principles of Tissue Engineering.

33. K.H. Leea, H.Y. Kimb, M.S. Khilb, Y.M. Rab, D.R. Leeb(2003).Characterization of nano-structured poly(1-caprolactone) nonwoven mats via electrospinning; Polymer 44,1287–1294.

34. Michael Jaffe, Zohar Ophir, Vaishali pai (2003). Biorelevant characterization of biopolymers; Thermochimica Acta 396,141-152.

35. Frank K. Ko. Nanofiber Technology: Bridging the Gap between Nano and Macro World Fibrous Materials Research Laboratory, Department of Materials Science and Engineering, Drexel University, Philadelphia, Pa. 19104, U.S.A